

DOE/BC/15209-2
(OSTI ID: 773362)

INCREASED OIL RECOVERY FROM MATURE OIL FIELDS USING
GELLED POLYMER TREATMENTS

Annual Report
June 16, 1999-June 15, 2000

By
G.P. Willhite
D.W. Green
C.S. McCool

Date Published: January 2001

Work Performed Under Contract No. DE-AC26-99BC15209

The University of Kansas
Center for Research, Inc.
Lawrence, Kansas



National Petroleum Technology Office
U.S. DEPARTMENT OF ENERGY
Tulsa, Oklahoma

DISCLAIMER

This report was prepared as an account of work sponsored by an agency of the United States Government. Neither the United States Government nor any agency thereof, nor any of their employees, makes any warranty, expressed or implied, or assumes any legal liability or responsibility for the accuracy, completeness, or usefulness of any information, apparatus, product, or process disclosed, or represents that its use would not infringe privately owned rights. Reference herein to any specific commercial product, process, or service by trade name, trademark, manufacturer, or otherwise does not necessarily constitute or imply its endorsement, recommendation, or favoring by the United States Government or any agency thereof. The views and opinions of authors expressed herein do not necessarily state or reflect those of the United States Government.

This report has been reproduced directly from the best available copy.

DOE/BC/15209-2
Distribution Category UC-122

Increased Oil Recovery from Mature Oil Fields Using Gelled Polymer Treatments

By
G.P. Willhite
D.W. Green
C.S. McCool

January 2001

DE-AC26-99BC15209

Prepared for
U.S. Department of Energy
Assistant Secretary for Fossil Energy

Thomas Reid, Project Manager
National Petroleum Technology Office
P.O. Box 3628
Tulsa, OK 74101

Prepared by
The University of Kansas Center for Research, Inc.
Tertiary Oil Recovery Project
1530 W. 15th St.
Lawrence, KS 66045-7609

Table of Contents

	<u>Page No.</u>
List of Figures	v
List of Tables	ix
Abstract	xi
Chapter 1 Introduction	1-1
Chapter 2 Determination of Aggregate Size during Gelation	2-1
Chapter 3 Effect of Added Acetate on the In Situ Gelation of the Polyacrylamide-Chromium(III) Acetate System	3-1
Chapter 4 Chromium(III) Transport in Carbonate Rock	4-1
Chapter 5 Pressure Distribution and Fluid Displacement in Gels	5-1
Chapter 6 Technology Transfer	6-1

List of Figures

<u>Fig. No.</u>	<u>Title</u>	<u>Page No.</u>
2.1	Schematic of channel for the flow field-flow fractionator.	2-2
2.2	Schematic of scattered light in cell of the multi-angle laser light scattering (MALLS) detector.	2-5
2.3	Schematic of dialysis cell.	2-6
2.4	Schematic of pumps and flow paths for FFFF channel.	2-7
2.5	Schematic of equipment for micro-batch runs using the multi-angle laser light scattering equipment.	2-8
2.6	Elution profiles from the FFF fractionator for a mixture containing 50, 100, 300, and 600 nm polystyrene particles.	2-11
2.7	Size distribution of a mixture containing 50, 100, 300, and 600 nm polystyrene particles.	2-11
2.8	Size distributions of two polystyrene sulfonate standards having molar masses of 990,000 and 2,613,000.	2-12
2.9	Elution profiles of Alcoflood 935 polyacrylamide for several amounts of injection mass.	2-13
2.10	Elution profiles for particles around or greater than one micrometer eluted under steric-flow mode.	2-14
2.11	Elution profiles of filtered and non-filtered Alcoflood 935 polyacrylamide samples.	2-15
2.12	Elution profiles of 5000 ppm Alcoflood 935 polyacrylamide and chromium(III) crosslinking gelant at several reaction times.	2-16
2.13	Size distribution of 5000 ppm Alcoflood 935 polyacrylamide and chromium(III) crosslinking gelant at several reaction times.	2-18
2.14	Zimm plot for measurements taken from the multi-angle laser light scattering detector on a 500k dalton dextran.	2-18
3.1	Schematic of apparatus for flow experiments.	3-2

<u>Fig. No.</u>	<u>Title</u>	<u>Page No.</u>
3.2	Flow resistance in sandpack during injection of gelant.	3-5
3.2	Flow resistance profiles in sandpack during injection of brine.	3-5
4.1	Schematic of equipment for flow experiments.	4-3
4.2	Absorbance scans of solutions used in study.	4-3
4.3	Normalized chromium concentration and pH in the effluent for alternate injection of chromium acetate solution (200ppm chromium; 1.0% KCl) and KCl brine; Core Bin#4.	4-5
4.4	Effect of flow rate on the normalized chromium concentration in the effluent during the injection of chromium acetate solutions (200ppm chromium; 0.5% KCl); Core Hong#3.	4-7
4.5	Effect of flow rate on the normalized chromium concentration in the effluent during the injection of chromium acetate solutions (200ppm chromium; 1.0% KCl); Core Hong#3.	4-7
4.6	Effect of KCl concentration on the normalized chromium concentration in the effluent during the injection of chromium acetate solutions (200ppm chromium); Core Hong#3.	4-8
4.7	Effect of shut-in time on the normalized chromium concentration in the effluent during the injection of chromium acetate solutions (200ppm chromium; 1.0% KCl); Core Hong#3.	4-9
4.8	Normalized chromium concentrations as functions of shut-in time, residence time and reaction time.	4-10
4.9	Recovery of pH during injection of brine after contact with a chromium acetate solution.	4-11
4.10	Effluent pH during the injection of a sodium acetate solution; Core Bin #4.	4-12
5.1	Schematic of equipment used for subjecting gels to a pressure gradient. (a) Experiments in 8-foot long tube. (b) Experiment in 5-foot long tube.	5-3
5.2	Pressures measured along the length of the gel-filled tube when pressure is applied to one end with brine and the opposite end of the tube is closed.	5-4

<u>Fig. No.</u>	<u>Title</u>	<u>Page No.</u>
5.3	Pressures measured along the length of the gel-filled tube when pressure is applied to one end with oil and the opposite end of the tube is open.	5-5
5.4	Schematic of the oil distribution in the gel in Section 1 of the tube.	5-6
5.5	Flow rate of oil during the period of time when oil penetrated the entire length of the gel.	5-7
5.6	Pressures measured along the length of the gel-filled tube when pressure is applied to one end with brine and the opposite end of the tube is open.	5-8
5.7	Pressures measured along the length of the gel-filled tube during the time period when brine developed channels through the gel.	5-9

List of Tables

<u>Table. No.</u>	<u>Title</u>	<u>Page No.</u>
2.1	Size distributions of two lots of Alcoflood 935 polyacrylamide that were determined by the equilibrium dialysis technique.	2-9
2.2	Size distributions measured with equilibrium-dialysis technique.	2-10
2.3	Molar mass and RMS radius for 500k dextran standard.	2-19
2.4	Molar mass and RMS radius for 200k polyacrylamide standard.	2-20
3.1	Permeabilities for the 40-ft sandpack in millidarcies.	3-3
4.1	Core Properties.	4-4
4.2	Material Balance on Chromium for Runs in Figure 4.3.	4-5

Abstract

Gelled polymer treatments are applied to oil reservoirs to increase oil production and to reduce water production by altering the fluid movement within the reservoir. This report describes the progress of the first year of a three-year research program. This program is aimed at reducing barriers to the widespread use of gelled polymer treatments by (1) developing methods to predict gel behavior during placement in matrix rock and fractures, (2) determining the persistence of permeability reduction after gel placement, and (3) developing methods to design production well treatments to control water production.

A technique using flow field-flow fractionation was developed to determine the size distribution of pre-gel aggregates that form during the gelation of a polymer system. Application of this technique to a polyacrylamide-chromium acetate system showed the aggregates became smaller in size with reaction time. This result was not expected and not consistent with measurements using an equilibrium dialysis procedure. Development of a third technique using a multi-angle laser light scattering detector was begun.

The bulk gel time of the polyacrylamide-chromium acetate system can be increased by the addition of acetate ions. The performance of an "added acetate" system was tested in a 40-foot long sandpack. It was demonstrated that the added acetate system can be propagated a distance of 40 feet over a time period of 160 hours without the development of increased flow resistance. The gelant did not form a gel through the length of the sandpack during an 18-month shut-in period. High flow resistance did develop in a portion of the pack during displacement after the shut-in period.

The propagation of chromium acetate solutions through dolomite rock was studied. Chromium retention increased with contact time with the rock. About half of the chromium was retained within five hours of contact time at the conditions investigated. The results demonstrate a problem that is encountered when applying polyacrylamide-chromium acetate system in-depth in carbonate rocks.

Work was conducted to determine pressure distributions and fluid displacements when a confined length of gel is subjected to a pressurized fluid at one end. The results show how oil and water develop channels and flow through gels.

Chapter 1

Introduction

Gelled polymer systems are applied to injection wells in mature oil fields for the purpose of in situ permeability modification to improve volumetric sweep efficiency in displacement processes such as waterflooding. Gelled polymers are also used to treat production wells to reduce water production and operating costs, prolonging the economic life of the wells. While the technology has been applied successfully, there are barriers to widespread utilization. These barriers generally involve a need to develop gel systems that can be used for in-depth treatment of matrix rock and a need for improved understanding of performance in matrix rock and fractures. This research program seeks to diminish these barriers through fundamental studies to predict gel behavior and placement in matrix rock and fractures and to develop a new approach to the control of water production in production wells.

The focus of studies for in-depth treatment in injection wells is the role of pre-gel aggregates, which form during the gelation process. The manner in which these aggregates affect gel placement will be mathematically modeled so that designs of treatments can be made more reliable. The application of treatments to injection wells in fractured reservoirs will be investigated by determining the effect of gel dehydration on the performance and persistence of gels that are placed in fractures. The approach to water control in production wells is based on two-phase flow characteristics of gelled polymer systems that are dehydrated in the reservoir rock after placement. Development of successful treatment strategies will provide the means for oil operators to reduce costs, since water production commonly represents a significant portion of oil field operational expenses.

This report presents most of the work that was accomplished during the first year of a three-year program. Graduate students performed the laboratory work as part of their requirements. Contributions of students are acknowledged at the beginning of each chapter.

Progress on the development of methods to measure the size distribution of pre-gel aggregates during the gelation of a polymer solution is reported in Chapter 2. A technique using Flow Field-Flow Fractionation (FFFF) was completed and results are presented for the polyacrylamide-chromium acetate gel system. Progress is presented on a second method to measure size distributions and molar masses of pre-gel aggregates. This method utilizes a multi-angle laser light scattering (MALLS) detector.

Supplying additional acetate ions to the polyacrylamide-chromium acetate system can extend the gel time of the system in bottle tests. The in situ performance of an "added acetate" system in a 40-foot long sandpack was investigated to determine the applicability of this system for in-depth treatments. Progress of this work is described in Chapter 3.

The propagation of chromium acetate solutions in carbonate rock was studied and the progress is reported in Chapter 4. Significant amounts of chromium were retained and the retention increased with the time the chromium acetate solution was in contact with the rock.

Work was conducted to characterize the phenomena that occur when a confined length of gel is contacted by a pressurized fluid at one end. Fluid displacements and pressure distributions along the length of the gel were determined and are reported in Chapter 5.

A listing of presentations and technical papers that present results from this work and work conducted in our previous DOE contract is given in Chapter 6.

Chapter 2

Determination of Aggregate Size during Gelation

Graduate Research Assistants: Pau Ying Chong, Tong Wang

Introduction

The polyacrylamide-chromium(III) gel system is used for gel treatments to control fluid movement in oil reservoirs by reducing the permeability of selected zones of the oil reservoirs. Control of the gel placement in the reservoir requires an understanding of the physical properties of the system during the gelation process. Gelation occurs by the crosslinking of polymer molecules by the chromium(III) ion. Previous work on polyacrylamide-chromium(VI)-thiourea system [McCool et al., 1991] showed that formation of pre-gel aggregates that grow in size to form a gel. The aggregates filter from the solution during flow through the reservoir rock. The retained aggregates develop significant flow resistance in the reservoir during gelant injection. In-depth placement of the gelant is retarded and difficult to control.

The objective of this study is to develop methods to determine the size distributions of pre-gel aggregates during the application of in-depth gelled polymer treatments. Size-distribution data are key to the prediction of permeability reduction during the placement of gelant in porous media. Permeability reduction is caused by the filtration/retention of aggregates. Two methods, equilibrium dialysis and flow field-flow fractionation (FFFF), were used to determine the size distributions of the pre-gel aggregates of a polyacrylamide-chromium acetate gel system as a function of reaction time. Preliminary runs using the FFFF equipment were also conducted with well-characterized samples in order to calibrate the procedures and to become familiar with the method. Initial work using a multi-angle laser light scattering (MALLS) detector was also conducted. The MALLS detector provides molar mass and size data on polymers in solution.

Background

Flow Field-Flow Fractionation. Flow field-flow fractionation (FFFF) is a technique that separates particles/molecules based on different diffusivities of different size particles/molecules [Giddings et al., 1986; Meyers, 1997]. The separation process of FFFF is conducted in a thin ribbon-like channel that is open and contains no packing material. A schematic of FFFF channel is shown in Figure 2.1. The sample is introduced into the channel through an injector valve and is carried through the channel by the carrier solvent stream. The top and bottom of the channel are fabricated from a porous ceramic frit, which allows a second solvent stream (crossflow) to flow across, perpendicular to the channel.

The crossflow stream is the driving force for sample retention. The crossflow stream forces the particles or polymer molecules in the sample to move toward the bottom of the channel which is called the accumulation wall. A semi-permeable membrane placed on the accumulation wall

allows for solvent passage but not passage of particles or large molecules in the sample. The particles/polymer-molecules diffuse back toward the center of the channel. The diffusion rates

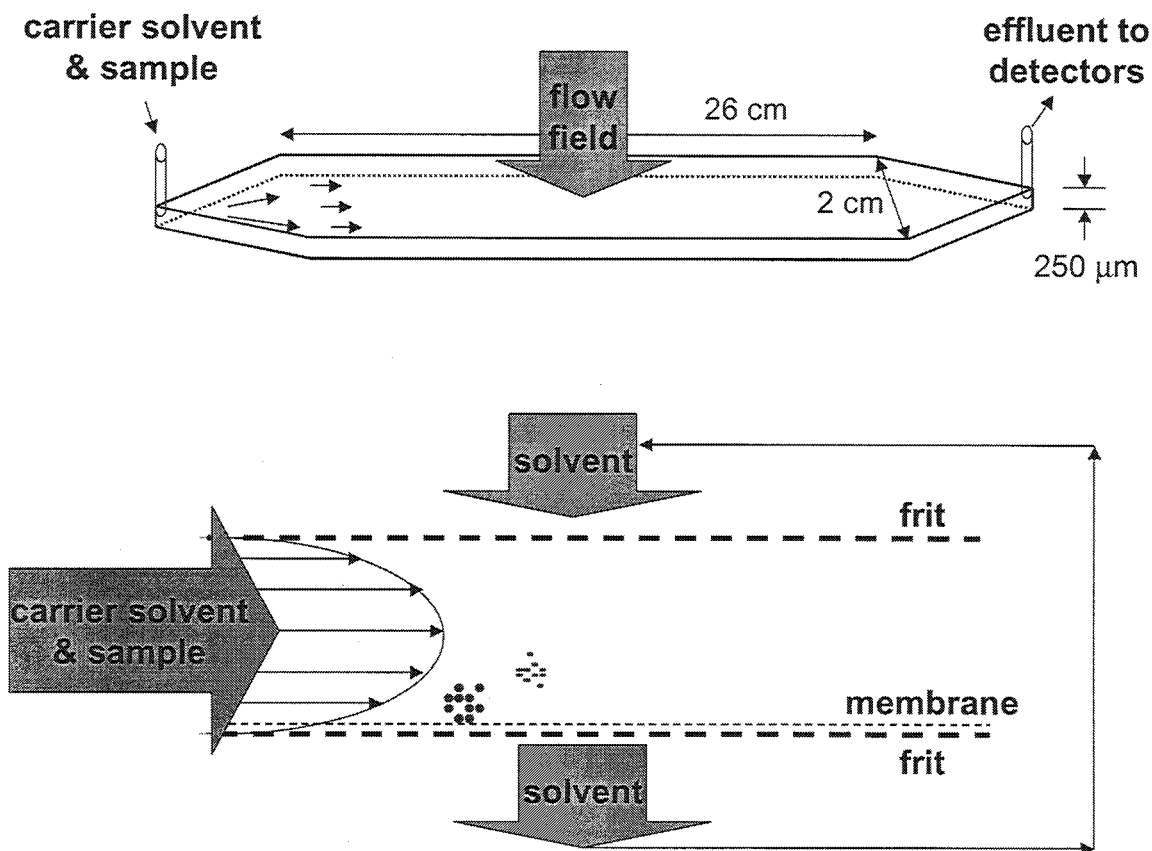


Figure 2.1 - Schematic of channel for the flow field-flow fractionator.

are related to the particle/polymer-molecule size. Smaller particles/polymer-molecules diffuse further from the wall. The particles/polymer-molecules form an exponential concentration distribution that is maximum at the accumulation wall and decreases towards the center of the channel at steady-state. The carrier-solvent flow stream is laminar and has a parabolic velocity profile where the flow velocity is zero at the wall and has a maximum value at the center of the channel. Differential elution of sample component occurs when the different axial flow velocities intercept the sample component with different concentration distributions. An inline UV detector attached to the channel outlet determines the mass of particles/polymer as a function of elution time from the fractionator.

The relationship between elution time and particle size is derived from theoretical models of the transport processes (laminar flow along the channel length, viscous drag and diffusion in the direction of the crossflow) and the Stokes-Einstein equation that relates particle size to the diffusion coefficient [Giddings et al., 1976]. Equation 2.1 is the relationship between particle diameter, d , and elution time, t

$$t = \frac{t^{\circ}}{\frac{2kTV^{\circ}}{\pi\eta dw^2 V_c} - 12 \left(\frac{kTV^{\circ}}{3\pi\eta dw^2 V_c} \right)^2} \quad \text{Eq. 2.1}$$

where,

- d = diameter of particle
- k = Boltzmann's constant
- t = elution time
- t[°] = time for non-retained particle to elute from channel (channel void volume/flow rate in channel)
- V[°] = channel void volume
- V_c = volumetric rate of crossflow
- w = channel thickness
- T = temperature
- η = viscosity of carrier liquid

Eq. 2.1 is applicable for particles or polymer molecules with diameters of approximately 1 μm or smaller. This cutoff size of 1 μm is dependent on the operating conditions. As the size of the particles/polymer-molecules become larger than the cutoff size, the separation mechanism in the channel undergoes a transition from normal FFFF to steric FFFF, where the size of the particle affects the concentration distribution from the accumulation wall. Large particles accumulate at the membrane and protrude into the stream where the flow is faster, eluting earlier than the theory predicts. Under this situation, calibration with standards of known size is necessary to relate sizes to elution times.

Modifications to the fractionator and operating procedures have improved the versatility and fractionating power of the method [Giddings, 1990]. A stop-flow procedure speeds the initial positioning the sample at the accumulation wall. The channel flow is stopped for a period of time after the sample has entered the channel allowing the crossflow to push the sample to the membrane. The frit outlet improves the detection capabilities by removing a significant portion of the effluent flow from the top of the channel. Only flow from the bottom of the channel next to the accumulation wall (which contains the sample) travels through the detector. The sample concentration is increased by this flow configuration.

Equilibrium Dialysis. The technique used to separate gel aggregates using membrane dialysis was modified from a technique developed by McCool et al. [1991]. An aqueous solution of a polydisperse polymer is placed in a reservoir that is separated from a reservoir of pure solvent by a membrane that contains pores of a given diameter. Polymer or aggregates on the sample side that are larger than the membrane pores are assumed to remain on the sample side during dialysis. Polymer or aggregates smaller than the membrane pores will diffuse through the membrane until the concentrations on both sides of the cell become equal. At equilibrium, the concentration of polymer on both sides of the membrane is determined and the amount of polymer/aggregates larger and smaller than the pore size is calculated. The dialysis technique is applied to a series of membranes having different pore sizes allowing for the determination of a quantitative size distribution.

Multi-Angle Laser Light Scattering. Light is scattered by polymer molecules as it travels through a solution containing the polymer. The amount and direction that the light is scattered provides information on the molecular weight and size of the molecule. The principal equation relating the light scattering to physical characteristics of the polymer molecule is:

$$\frac{R(\theta)}{K^*c} = M_w P(\theta, r_g^2) - 2A_2 M_w^2 P^2(\theta, r_g^2) c \quad \text{Eq. 2.2}$$

where,

- $R(\theta)$ = excess Rayleigh ratio; a measure of the fraction of light intensity that is scattered by the polymer molecule (a function of the scattering angle)
- K^* = light-scattering constant containing the wavelength of the incident light, the refractive index of the solvent, the refractive index increment (dn/dc) and other physical parameters and constants
- c = concentration of polymer
- M_w = weight-average molar mass
- $P(\theta, r_g^2)$ = scattering function (and is a function of the scattering angle and the mean square radius of the molecule)
- A_2 = second virial coefficient
- r_g^2 = mean square radius
- θ = scattering angle.

Wyatt [1993] and Huglin [1972] describe theory and measurement techniques of light scattering in detail. A light scattering experiment consists of measuring the amount of scattered light from a sample at various angles as shown in Figure 2.2. The polymer concentration must be known or measured by another detector. Other constants such as the refractive index of the solvent and the refractive index increment, dn/dc , must also be known or measured. The light scattering data along with the other known or measured parameters are used in Eq.2.2 along with specialized plotting techniques to determine the molar mass and the root-mean-square (RMS) radius of the polymer sample.

Two types of light scattering experiments are performed depending on whether the sample is fractionated or not fractionated. In batch mode when the sample is not fractionated, light scattering data are taken on samples that are prepared at a series of known concentrations. The data are displayed on a Zimm plot. Extrapolation of the data on the Zimm plot to a zero scattering angle and to zero concentration allows for the determination of the weight-average molar mass and the RMS radius of the polymer. Examples of this mode of operation are described in this chapter.

The light scattering detector can also be used to take measurements on polymer samples that have been fractionated by size-exclusion chromatography or flow field-flow fractionation. This inline mode of measurement requires an additional inline detector (UV or RI) to provide concentration data. The light scattering and concentration data are then displayed on a Debye

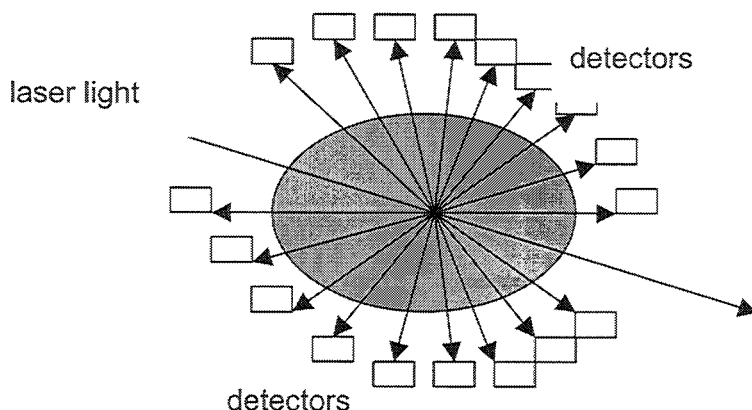


Figure 2.2 – Schematic of scattered light in cell of the multi-angle laser light scattering (MALLS) detector.

plot and extrapolated to zero angle to give the molar mass and mean square radius for each slice of eluting polymer from the fractionator. Summing all of the slices during an eluting peak provides the determination of molar mass and size distributions. It is planned to implement the inline mode of operation during the next year of work.

Experiment

Equilibrium Dialysis. The procedure for determining size distributions using equilibrium dialysis is long and tedious which is the reason for developing an alternate method. A schematic diagram of a dialysis cell is shown in Figure 2.3. The cells were made from Teflon™ stock and constructed in house. Each half-cell contains a reservoir that is 1.5 inches in diameter and 0.125 inches deep. When assembled, a polycarbonate membrane that contained precision cylindrical pores separates the reservoirs. A confining apparatus holds the cells together. A series of pore diameter were used (50, 100, 200, 400, 600, 800, 1000 nm) to produce a size distribution.

The general procedure for the equilibrium-dialysis technique used on polymer solutions and on reacting gelants is described. The sample was first diluted in order to quench the gelation reactions. After a specified reaction time, the reacting gelant was diluted by a factor of 10 by adding 1% KCl, the solvent used to prepare the gelant. The second step was a tubing dialysis procedure that was conducted to reduce the chromium concentration. The diluted sample was placed in a 12,000-to-14,000 molecular-weight-cutoff (MWCO) dialysis tubing and dialyzed against more solvent (1% KCl) for two days. The sample to solvent ratio was 1:30. The pore size for the dialysis tubing is approximately 2.5 nm. The polymer or gel aggregates will not pass through the tubing but the unreacted chromium will dialyze from the sample to the solvent. After the dilution and tubing dialysis steps, the concentration of the polymer was reduced to 500 ppm and the unreacted chromium concentration was reduced by a factor of approximately 300 to a value less than 1 ppm. These steps effectively quench the gelation reactions.

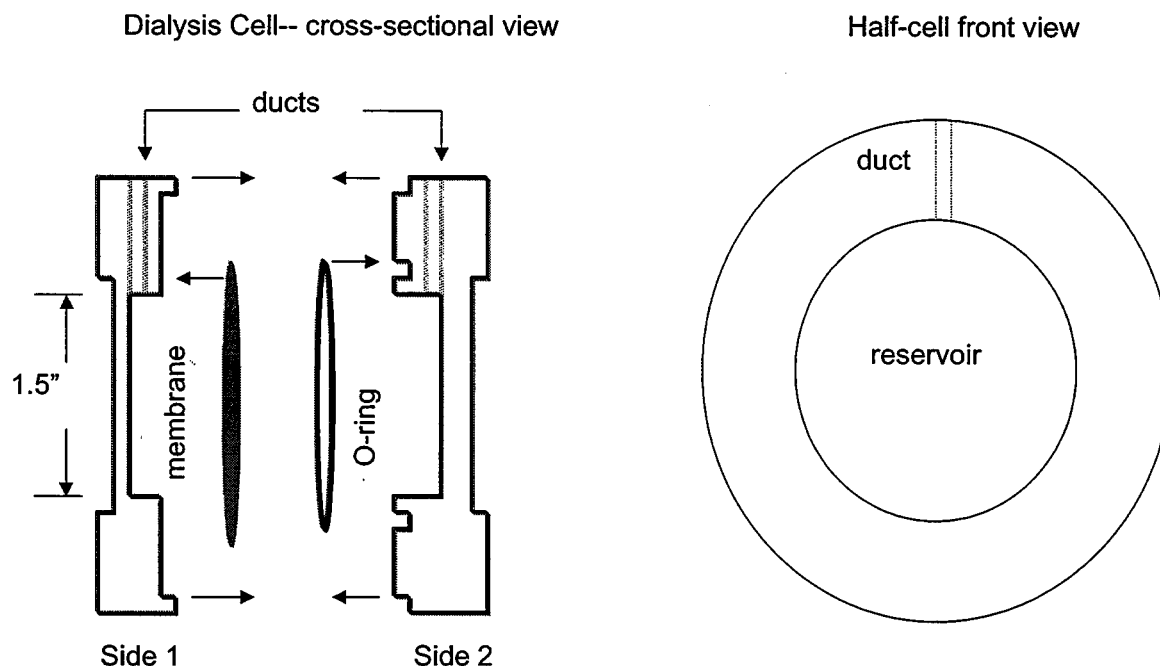


Figure 2.3 - Schematic of dialysis cell.

The sample was ready for the polymer dialysis step after removal from dialysis tubing. 2.5 mL of sample was charged to one side of the dialysis cell and 2.5 mL of solvent (1% KCl) was charged to the other side. The KCl solution was filtered through a 0.22 μm membrane to eliminate impurities. Plugs sealed the access ducts of the cells and the cells were placed in a 30°C waterbath for a two-week dialysis time. The two-week time period was selected as necessary for a close approach to equilibrium. After the two-week dialysis, the solutions from both sides of the dialysis cell were removed and the polymer concentrations were determined by UV absorption.

The amount of polymer smaller than the membrane pore size is twice the amount of polymer that diffuses through the membrane. This calculation assumes that the polymer that is smaller than the pore size evenly distributes on both sides of the membrane and that the polymer larger than the pore size remains on the sample side. Material balances on the sample charged and removed from the cells were calculated to insure the integrity of the experimental procedure.

Flow Field-Flow Fractionation. Experiments were conducted with a Model F-1000 FIFO Universal Fractionator (FFFractionation, LLC; Salt Lake City, UT). The channel dimensions were 2.0 cm wide, 28 cm long and 0.0141 cm thick. The channel was equipped with a frit outlet. Three pumps were required for operation as shown in Figure 2.4. The channel flow pump provided flow through the sample injection valve, the channel and the detector. A second pump was configured to control flow out of the frit-outlet. The frit outlet and corresponding pump are used to draw a significant portion of the flow from the upper portion of the channel which does

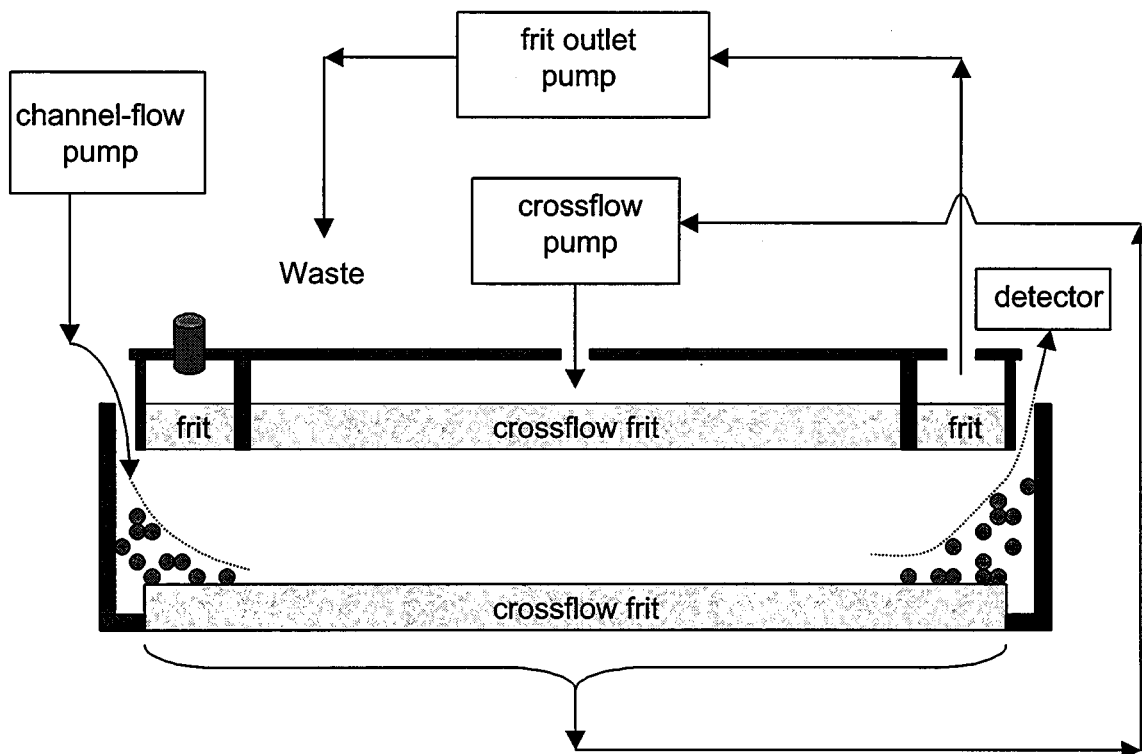


Figure 2.4 - Schematic of pumps and flow paths for FFFF channel.

not contain the sample. This allows the sample that exits the channel to be more concentrated in the UV detector. A third pump was configured in a loop to control the inlet and outlet flow of the crossflow stream.

Samples were introduced with an injection valve equipped with a 10 μL sample loop. Material eluted from the channel was measured using a Waters 490 UV detector. Data were collected during a run by computer using the Flow-160 program (FFFractionation, LLC; Salt Lake City, UT). Data were analyzed on a computer using the FFF Analysis program (FFFractionation, LLC).

Multi-Angle Laser Light Scattering. Light scattering measurements were conducted with a Dawn EOS Light Scattering Instrument (Wyatt Technology Corp., Santa Barbara, CA) that was configured in microbatch mode as shown in Figure 2.5. Solvent is continuously pumped through the instrument at a flow rate of 0.5 mL/min. Samples of polymer prepared at several known concentrations are inserted into the flow stream using an injection valve fitted with a 0.91-mL sample loop. The computer program ASTRA (Wyatt Tech. Corp) was used to collect and process the light-scattering data.

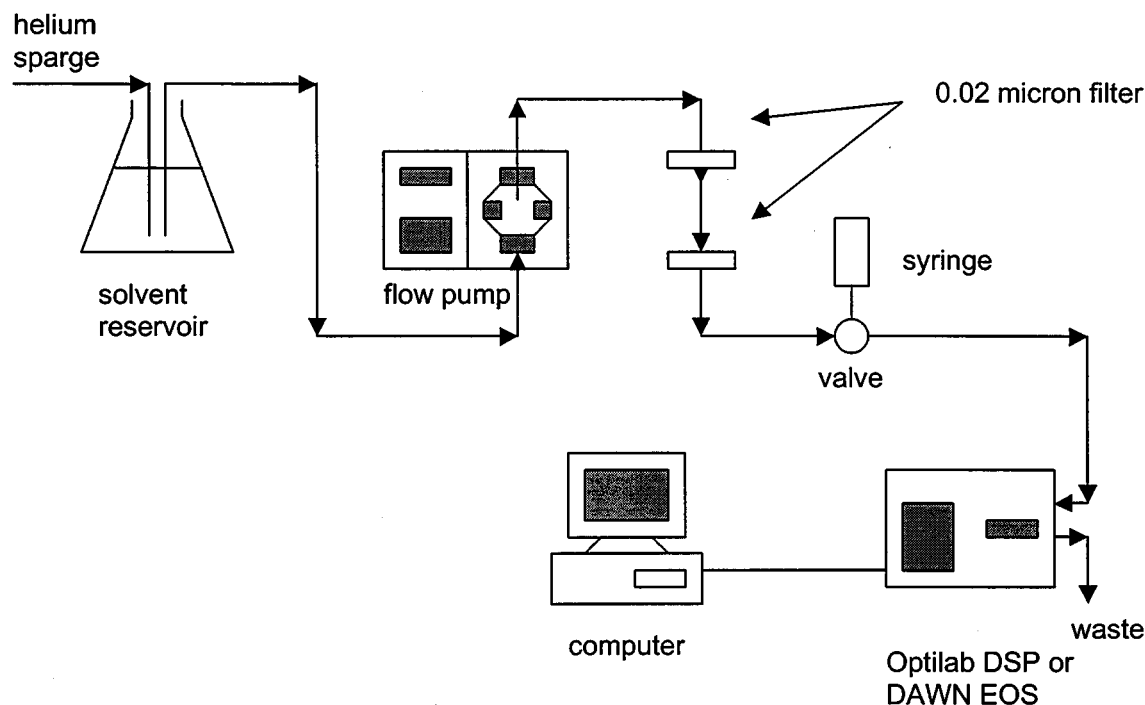


Figure 2.5 – Schematic of equipment for micro-batch runs using the multi-angle laser light scattering equipment.

Runs were also conducted using the same procedure described above but using the Optilab DSP interferometric refractometer instrument and DNDC software (Wyatt Tech.Corp.). These measurements provide the specific refractive index increment, dn/dc , which is the change of refractive index with the concentration of polymer. Densities of the polymer solutions and the refractive index of the solvent were also measured. These measured values are required for the determination of molar mass and size parameters from the light scattering data. All of the instruments used were calibrated according to manufacture's procedures.

Materials The gel system selected for study contained 5000 ppm Alcoflood 935 polyacrylamide, 100 ppm chromium (from a 50% chromium acetate solution; McGean and Rhoco, Inc., Cleveland, OH) and 1.0% KCl. Two lots of polymer were used. The nominal gel times at 25°C were 11 hours and 45 hours for Lots 3243A and 7158V, respectively. The initial viscosities of the gel systems were 43 cp and 25 cp (shear rate = 22.5/s) for Lots 3243A and 7158V, respectively. These measurements indicated that the average molar mass of Lot 3243A was greater than the average molar mass of Lot 7158V. Equilibrium dialysis measurements were conducted on both lots and flow field-flow fractionation (FFFF) measurements were conducted on Lot 7158V. The carrier solvent for all flow streams through the FFFF system for analyses of the gel system was water containing 1 wt% potassium chloride.

Calibration standards were also measured on the FFFF system. Polystyrene latex spheres with diameters of 50, 100, 300, 600, 900, 2000, 5000, and 10,000 nm were obtained from Duke Scientific. Polystyrene sulfonate sodium salt (PSS) samples were obtained from Polymer Standards Service-USA, Inc. The molar masses of the PSS standards were 990,000 and 2,613,000 daltons. The carrier solvent for all flow streams was water containing 0.02 wt% sodium azide (bactericide), 20 mM sodium phosphate (buffer agent) and 0.1 wt% FL-70 (surfactant). The solvent was degassed and filtered through a 0.22 μm membrane prior to use.

The multi-angle laser light scattering instrument was tested by analyzing two water-soluble polymers. A dextran standard having a molar mass of 500k daltons was prepared in water containing 100 ppm sodium azide. A polyacrylamide sample was prepared in water containing 1.0 wt.% KCl and 100ppm sodium azide. The polyacrylamide was obtained in 1989 and labeled as having a molar mass of 200k daltons.

Results and Discussion

Equilibrium Dialysis. Size distributions were determined by equilibrium dialysis for polymer solutions without crosslinker. The size distributions for solutions prepared from two lots of polymer are shown in Table 2.1. The polymer molecules are larger in Lot 3243A than in Lot 7158V. This is consistent with the observation that Lot 3243A has a higher viscosity and faster gelation time than Lot 7158V at the same conditions.

Table 2.1 - Size distributions of two lots of Alcoflood 935 polyacrylamide that were determined by the equilibrium dialysis technique.

Size range (nm)	Polymer solution Lot 3243A (wt%)	Polymer solution Lot 7158V (wt%)
0 – 100	15	43
100 – 200	24	34
200 – 400	36	14
400 – 600	18	6
600 – 800	2	0
> 800	5	1

Size distributions were determined by equilibrium dialysis for gelants that were allowed to react for ten minutes and 9 hours. Lot 3243A polymer was used to prepare the gelant. The nominal gel time for the system was about 11 hours. Size distributions for the polymer without crosslinker and for the gelant are given in Table 2.2. The data show little growth in the size of the molecules/aggregates during the first ten minutes after the crosslinker was added to the polymer solution. Molecules/aggregates grew to larger sizes as shown by the gelling reaction for a 9 hours old gel. The growth in size of the aggregates was not dramatic even though the 9-hour old gelant was close to the gel time of the system. Experimental procedures were checked using material

balances that were calculated as the percentage of the amount of polymer removed from the cell with respect to the amount charged. The material balances were 102% \pm 3%.

Table 2.2 – Size distributions measured with equilibrium-dialysis technique.

Size range (nm)	Size Distribution (wt.%)		
	Polymer solution (Lot 3243A)	Gel 10-minute old	Gel 9-hour old
0 – 100	15	15	17
100 – 200	24	27	24
200 – 400	36	34	28
400 – 600	18	15	17
600 – 800	2	6	3
> 800	5	3	11

Flow Field-Flow Fractionation (FFFF). Experiments were conducted to test and to develop procedures for the FFFF system to fractionate samples. Runs were conducted with polystyrene standard spheres that have narrow size distributions and polystyrene sulfonate standards. Size distributions were then determined for an Alcoflood 935 polyacrylamide solution and a gelant that contained Alcoflood 935 polyacrylamide and chromium acetate.

Fractionation of polystyrene particle standards. Many runs were conducted on samples that contained polystyrene particles of different size. Polystyrene is not water-soluble so the polymer remains as a spherical particle in aqueous solution. An example of a run for a mixture of polystyrene particles having diameters of 50, 100, 300 and 600-nm is shown in Figure 2.6 where the response of the UV detector is plotted as a function of time. The data show that the polystyrene particles of this particular size range can be separated in less than one hour. The data from Figure 2.6 were converted to a size distribution using FFFF theory and are shown in Figure 2.7. The identities of each peak were established through separate runs using only one or two components at a time. There is good agreement between the calculated diameter and cited diameter from manufacturer. The relative mass values in Figure 2.7 are incorrect since the relationship between mass and the UV response from the detector is not known for particles. Experiments on the spherical particles indicate that the FFFF is a viable method to determine the size distribution of pre-gel aggregates.

Fractionation of polystyrene sulfonate standards. Sulfonated polystyrene is water-soluble and the size of the molecules in aqueous solution depends on the characteristics of the solvent. Size distributions for two FFFF runs on samples containing two different molar mass polystyrene sulfonate standards in a 1% KCl solution are shown in Figure 2.8. The average diameters, determined at the peak response, for the 990,000 and 2,613,000 MW polystyrene sulfonate in 1% KCl solution were determined as 63 and 133 nm, respectively.

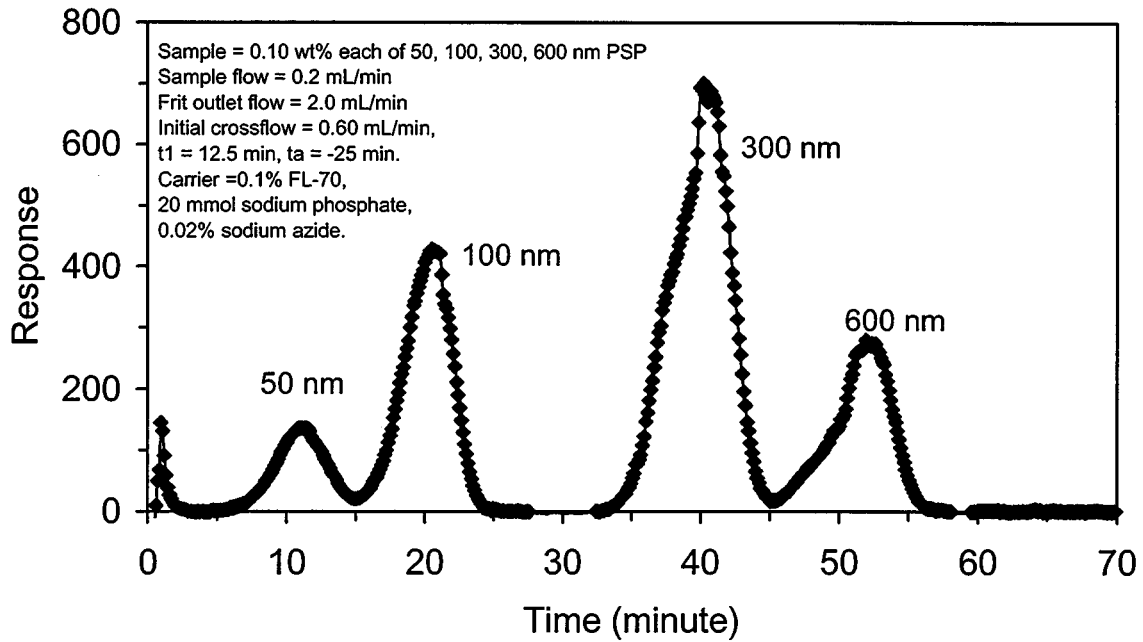


Figure 2.6 - Elution profiles from the FFF fractionator for a mixture containing 50, 100, 300, and 600 nm polystyrene particles.

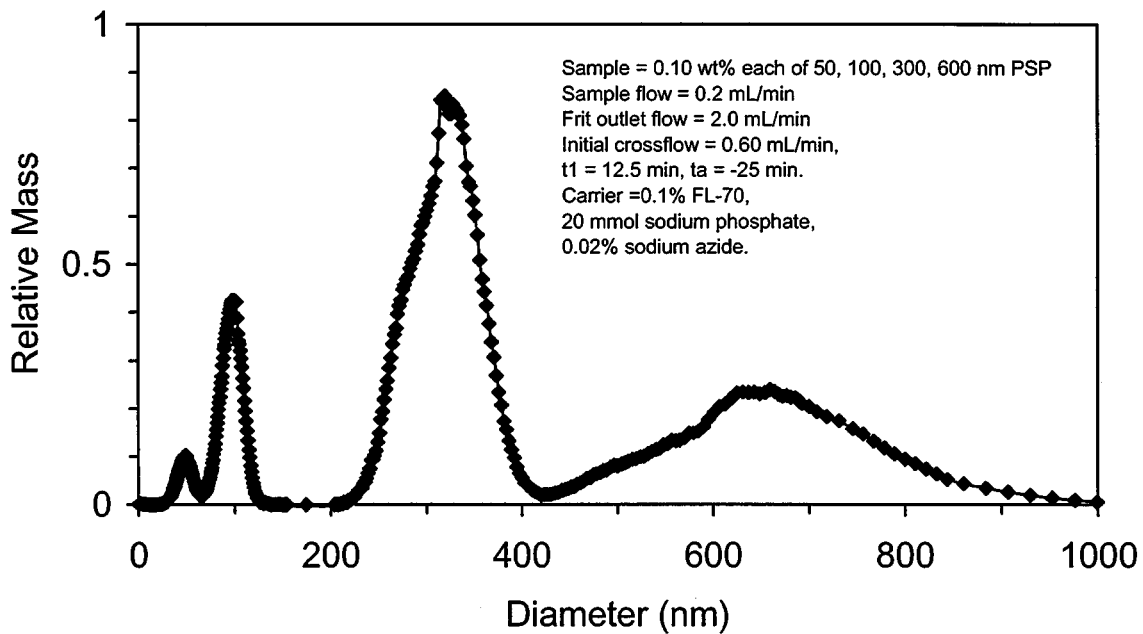


Figure 2.7 – Size distribution of a mixture containing 50, 100, 300, and 600 nm polystyrene particles

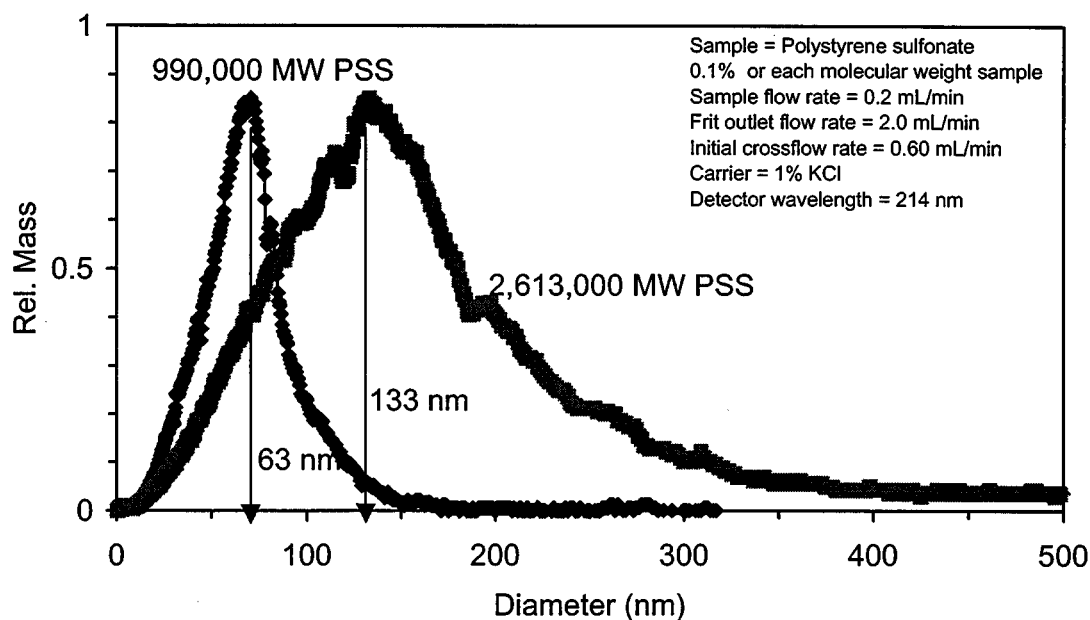


Figure 2.8 – Size distributions of two polystyrene sulfonate standards having molar masses of 990,000 and 2,613,000

Diameters of the polystyrene sulfonate standards were also calculated using the relationship that is derived from the Mark-Houwink-Sakurada equation and the Einstein's viscosity equation.

$$d = \sqrt[3]{\frac{12KM^{a+1}}{5N_0\pi}}, \quad \text{Eq. 2.3}$$

where d is the hydrodynamic diameter, M is the molar mass, N_0 is the Avogadro's number (6.023×10^{23} /mol) and K and a are fitting parameters. The K and a values used were 17.8×10^{-3} mL/g and 0.68, respectively, [Kurata and Tsunashima, 1999]. These values were for a solvent containing 0.10 M NaCl, similar to the 0.134M (1%) KCl used in the FFFF runs. The equivalent diameters calculated for the 990,000 and 2,613,000 MW polystyrene sulfonates were 64 and 111 nm, respectively. These values compare well with the experimental results of 63 and 133 nm obtained from the FFFF runs.

Fractionation of Alcoflood 935 polyacrylamide. The size distribution of Alcoflood 935 polyacrylamide (Lot 7158V) was determined by flow field-flow fractionation (FFFF). Additional runs were conducted to verify that the experimental parameters used were consistent with the separation theory and the mathematical models. Figure 2.9 shows the UV response as a function of time for different polymer loadings in the injected sample. Loading is the mass of sample

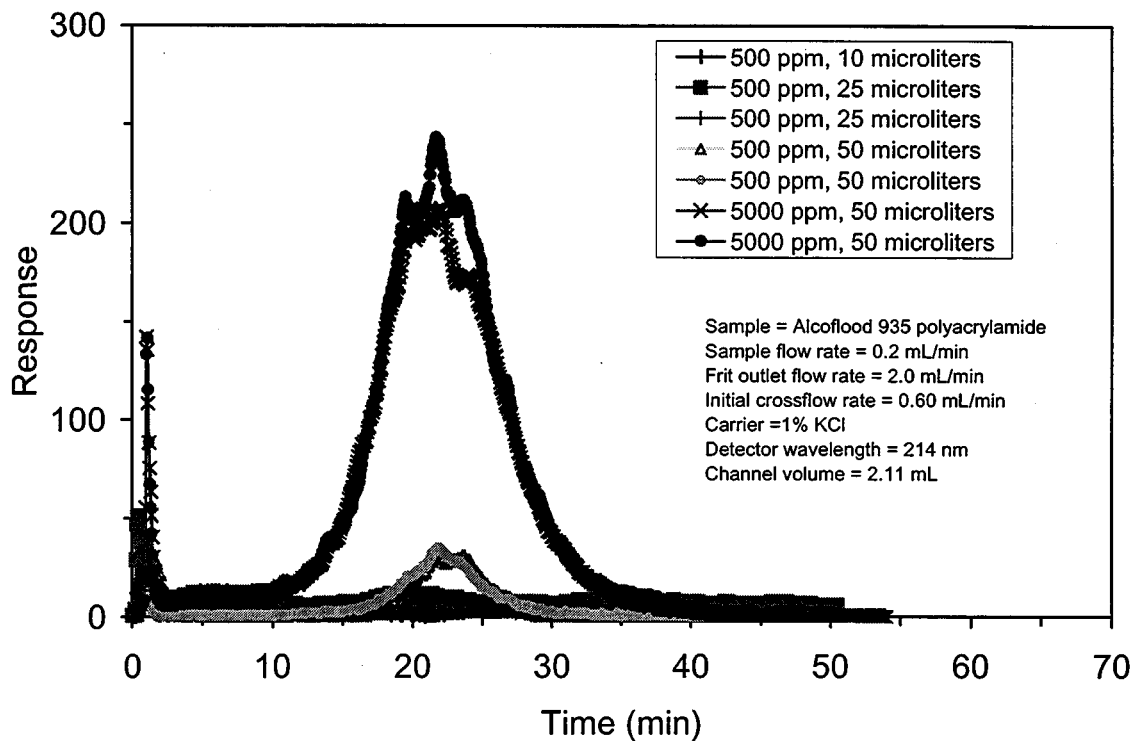


Figure 2.9 - Elution profiles of Alcoflood 935 polyacrylamide for several amounts of injection mass.

injected and is the product of the concentration and the sample size. A loading that is too high can skew the elution profile. The elution characteristics shown in Figure 2.9 are independent of the amount of sample injected up to 250 μg . A 50 μg sample loading was used for most runs.

The average diameter of the molecules in Alcoflood 935 polyacrylamide is in the range of 140 to 170 nm. This diameter range is based on the elution time of the sample peak (18 to 24 minutes) in Figure 2.9 and *normal* flow field-flow fractionation theory.

As described in the following section, a question arose as to whether the diameters of the Alcoflood 935 molecules were submicron and thus eluted the FFFF channel in the manner described by *normal* FFFF theory or that the diameters were supra-micron and exhibited steric flow in the channel. Larger sizes elute faster during steric flow as opposed to eluting later during *normal* flow. The size of the polyacrylamide molecules under steric flow conditions is determined through the use of a calibration. The calibration is determined by injecting particles with known diameters at the same flow conditions and determining the elution times as shown in Figure 2.10. Inspection of the data in Figure 2.10 show that the diameter of the Alcoflood 935 molecules would be between 2000 to 5000 nm based on steric flow conditions. It is unlikely that

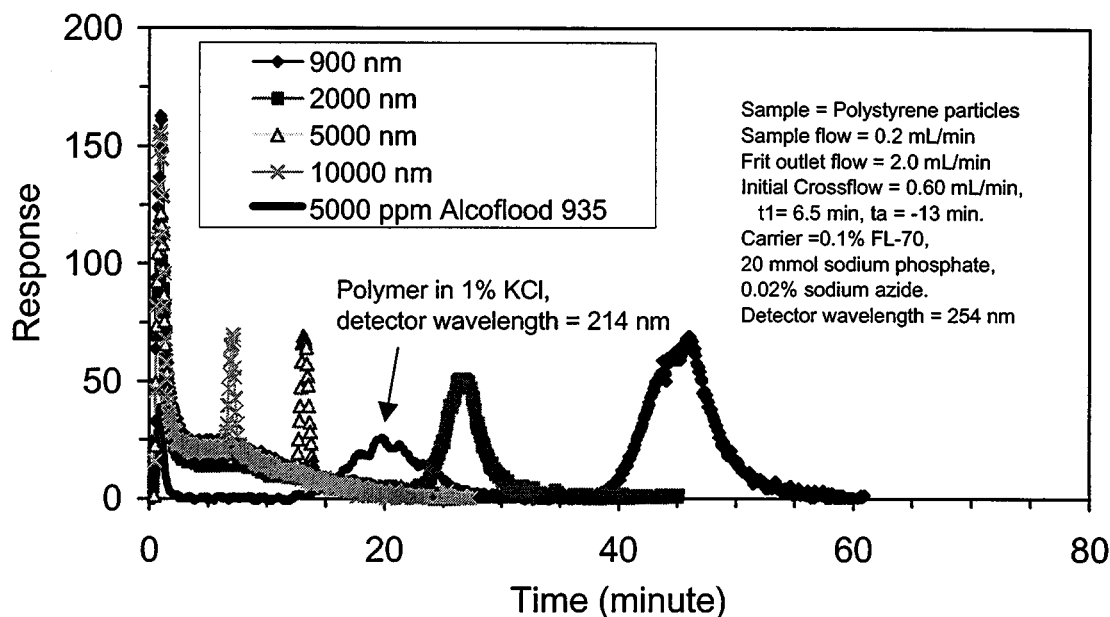


Figure 2.10 – Elution profiles for particles around or greater than one micrometer eluted under steric-flow mode.

diameters based on steric flow are correct since the results of the equilibrium dialysis experiments showed that the size of the Alcoflood 935 molecules (Lot 7158V) ranged from 0 to 600nm.

Additional FFFF runs were conducted to confirm the size that was determined for the Alcoflood 935 molecules. A 5000 ppm polymer solution was filtered through a 500 nm filter prior to injection into the FFFF channel. Figure 2.11 shows the elution profiles for polymer solutions that were filtered and unfiltered. Little change between the elution profiles indicates that the polymer is smaller than 500 nm and therefore follows the *normal* flow field-flow fractionation theory.

Additional evidence showed that the diameters of Alcoflood 935 molecules that were calculated by *normal* FFF theory were reasonable values. Hecker et al. [1999] used multi-angle laser light scattering and determined the diameters of polyacrylamide standards having molar masses of 1.14×10^6 , 5.55×10^6 , and 9.00×10^6 to be 62, 103, and 136 nm, respectively. These values are consistent with measured values of 140 to 170 nm for Alcoflood 935 with a reported molar mass of 5×10^6 .

Diameters of Alcoflood 935 molecules were also determined in our laboratory by measuring the intrinsic viscosity of the polymer solution. The intrinsic viscosity of Alcoflood 935 (batch # 7158V) was 970 mL /g. The hydrodynamic diameter was calculated from the following form of the combination of Einstein's Viscosity Equation and the Mark-Houwink-Sakurada equation:

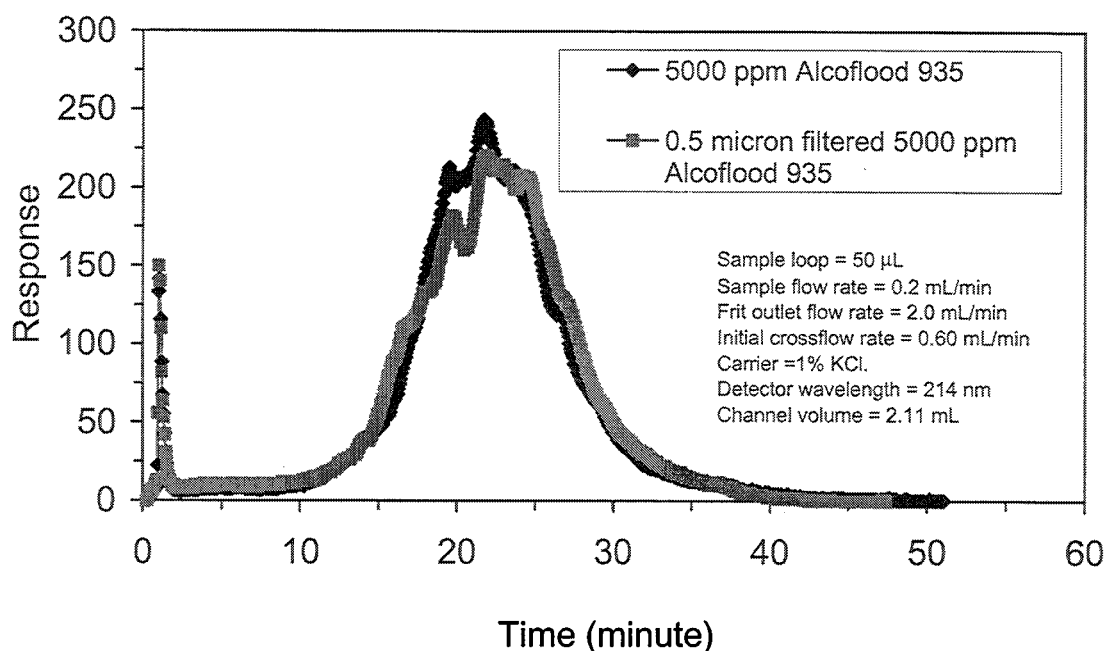


Figure 2.11 - Elution profiles of filtered and non-filtered Alcoflood 935 polyacrylamide samples.

$$d = \sqrt[3]{\frac{12[\eta]^{1+1/a}}{5N_0\pi K^{1/a}}} \quad \text{Eq. 2.4}$$

where d is the hydrodynamic diameter, $[\eta]$ is the intrinsic viscosity, N_0 is the Avogadro's number (6.023×10^{23} molecules/mole) and K and a are fitting parameters. The K and a values used were 3.73×10^{-2} mL/g and 0.66, respectively, as reported by the manufacture (Ciba Specialty Chemicals, USA; Suffolk, Virginia). The calculated hydrodynamic diameter was 182 nm. These additional measurements strongly support the values of diameter determined from the FFFF measurements that are analyzed by *normal*-flow theory.

Fractionation of reacting gelant. Size distributions of the polymer-molecules/aggregates in the Alcoflood 935 polyacrylamide-chromium(III) system during the gelation process were determined by FFFF. Elution profiles at different reaction times are shown in Figure 2.12. A shifting of the elution profiles to lower retention times as a function of reaction time was observed. Smaller molecules/aggregates elute sooner than larger molecules/aggregates when fractionation in the channel occurs under *normal* FFFF conditions, that is, when the size of the molecules/aggregates are less than about 600 nm. Based on the *normal* FFFF theory, the shifting to lower retention times with reaction time indicates that the molecules/aggregates are becoming smaller as the gelation reactions proceed. This result was unexpected and contrary to data obtained from the equilibrium dialysis experiments where the size of the molecules/aggregates grew with reaction time.

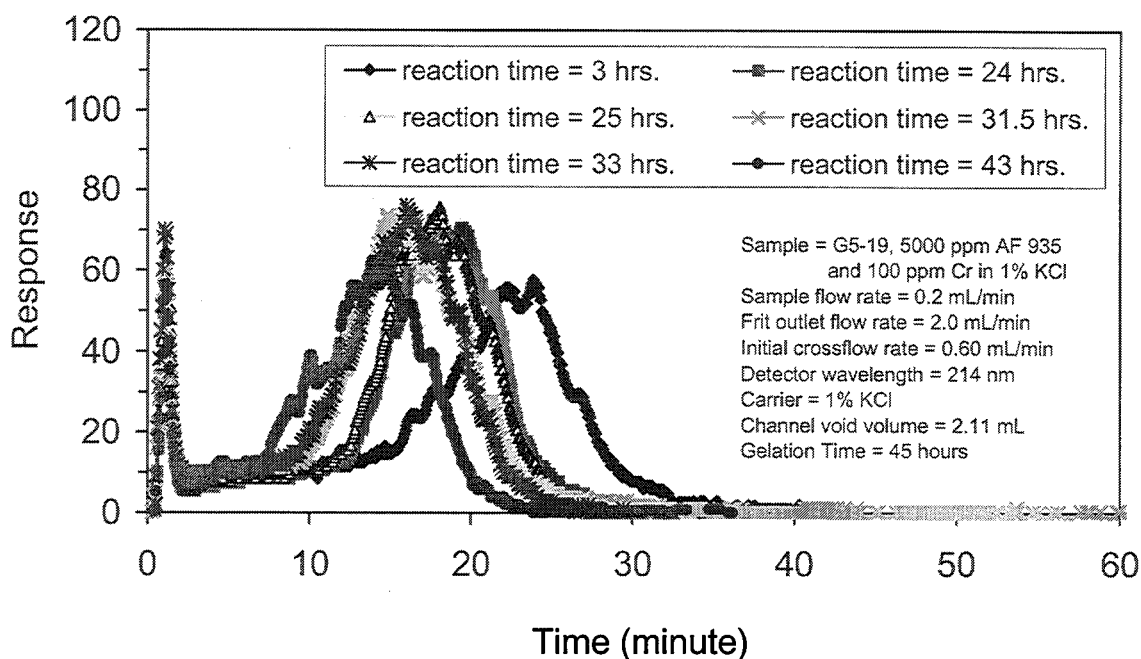


Figure 2.12 - Elution profiles of 5000 ppm Alcoflood 935 polyacrylamide and chromium(III) crosslinking gelant at several reaction times.

Work was conducted to verify that the data from the FFFF runs, and the interpretation thereof, were correct. Data obtained for the FFFF runs on the gelling system were reproducible. Runs conducted with samples of polymer without crosslinker were conducted in between runs conducted on the reacting gel system. Elution times for runs conducted on polymer solutions without crosslinker were consistent and were comparable to runs conducted on the freshly prepared gel system. These additional runs verified that the data obtained from the reacting gel system were accurate.

Interpretation of the data from FFFF runs can be ambiguous without supplemental data. During *normal* FFFF, molecules/aggregates elute at later times as their size increases up to about 600 nm in diameter. As the size increase above 600 nm, steric FFFF occurs and the elution time decreases. Thus, two diameters are represented at a particular elution time, one for *normal* flow and one for steric flow. The diameter based on *normal* flow is predicted by theory and is calculated by software that accompanies the FFFF equipment. Diameters based on steric flow are determined by calibration with particles of known diameters. Work conducted on the polymer without crosslinker and described in the previous section showed that the polymer molecules were fractionated under *normal* flow conditions and the average diameter of the polymer molecules was about 170 nm. The diameter of the molecules/aggregates of the freshly-prepared gel system was also about 170 nm since the elution times for runs on the freshly-prepared gel system were comparable to runs conducted on polymer solutions without crosslinker. It is unlikely that the addition of crosslinker to the polymer increased immediately the diameters of the molecules/aggregates to the 2000 – 5000 nm range and that the elution times just happened to

coincide. It is much more likely that the reacting gel system was fractionated under *normal* flow conditions and that the initial average diameter of the molecules/aggregates was about 170 nm.

The initial results from the FFFF runs indicate that the polymer aggregates decrease in size as the gelation reactions proceed. It is plausible that the aggregates become more compact due to intramolecular crosslinks. At some point during gelation, intermolecular crosslinks must become significant to bond the aggregates together and form a three-dimensional gel. The FFFF runs were conducted on samples at reaction times less than the nominal gel time. The nominal gel time was determined from viscosity measurements that remained relatively constant for a period of time and then increased sharply with time. The gel time was defined as the when the viscosity of the system was greater than 1000 cp during the period of sharply increasing viscosity. At the gel time, the system is still relatively fluid and it takes several more hours for further development of gel structure. It is possible that FFFF runs on samples after reacting for times greater than the nominal gel time might show increases in aggregate size.

It was established and discussed in a previous section that the Alcoflood 935 polymer aggregates are smaller than one micrometer and the average diameters are in the range of 100 to 200 nm. The polymer molecules fractionate under *normal*-flow mode and the retention time will directly relate to its size based on normal FFF theory. Data presented in this section have shown the reacting gelant initially has the same elution characteristics as the non-reacting polymer solution. As the gelation reaction proceeds, the systematic shifting of the gelant elution profile to the lower retention time suggested that the gelant aggregates become smaller. This trend is reproducible. Size distribution profiles as a function of reaction time are shown in Figure 2.13.

The shear environment experienced by the gelant samples during analysis in the flow field-flow fractionator might affect the size of the polymer molecules/aggregates. Work will be conducted to determine the effect of the shear environment on the size of molecules/aggregates. Application of the multi-angle laser light scattering detector will enhance our ability to measure molecule/aggregate sizes.

Multi-Angle Laser Light Scattering. Preliminary measurements using the multi-angle laser light scattering (MALLS) detector were completed. Molar masses and root-mean-square (rms) radii were determined for two polymers, dextran and polyacrylamide.

A dextran polymer having a reported molar mass of 500,000 daltons was measured in the MALLS detector using the batch procedure. An example of the analyzed data in the form of a Zimm plot is presented in Figure 2.14. A term composed of the light scattering intensity and concentration, $[K \cdot c / R(\theta)]$, is plotted as a function of a term that is composed of the scattering angle and concentration, $[\sin^2(\theta) - \text{constant} \times c]$. The constant in the abscissa term is selected to spread the data on the plot. The Zimm plot is constructed in order to extrapolate the data to zero concentration at a zero scattering angle. In this example, four concentrations of the polymer were measured at 14 angles and the data are plotted in Figure 2.14 as small circles. For each concentration, lines were regressed through the 14 angles and extrapolated to zero scattering angle. For each scattering angle, lines were regressed through the four concentrations to a zero concentration. The extrapolated values are plotted as squares. The weight average molar mass for

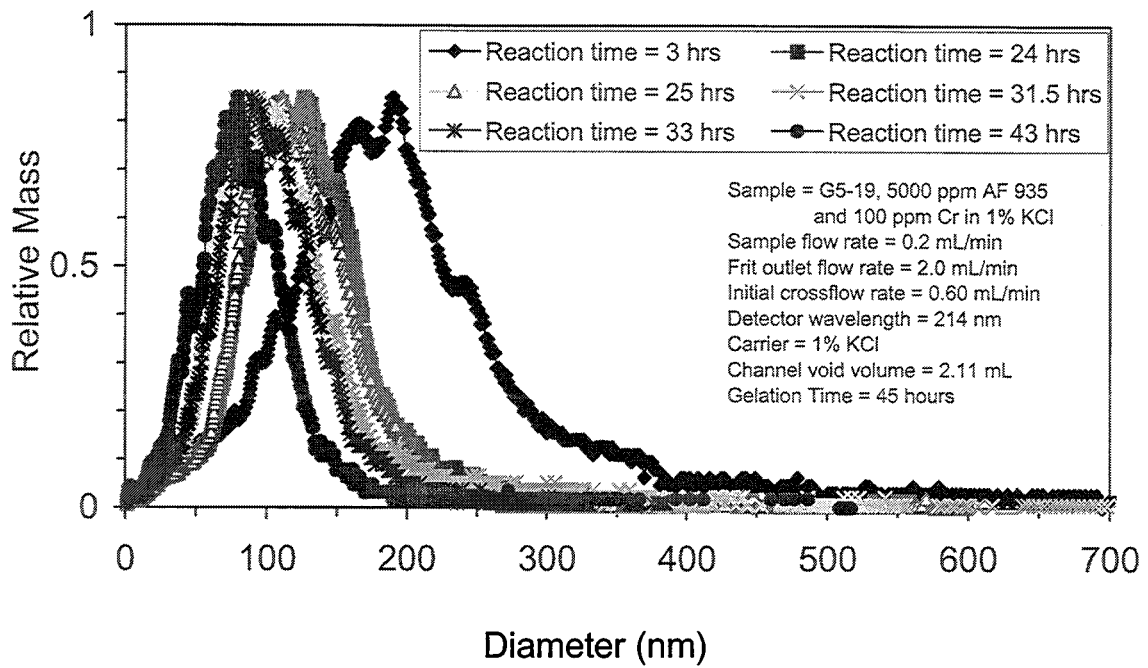


Figure 2.13 - Size distribution of 5000 ppm Alcoflood 935 polyacrylamide and chromium(III) crosslinking gelant at several reaction times.

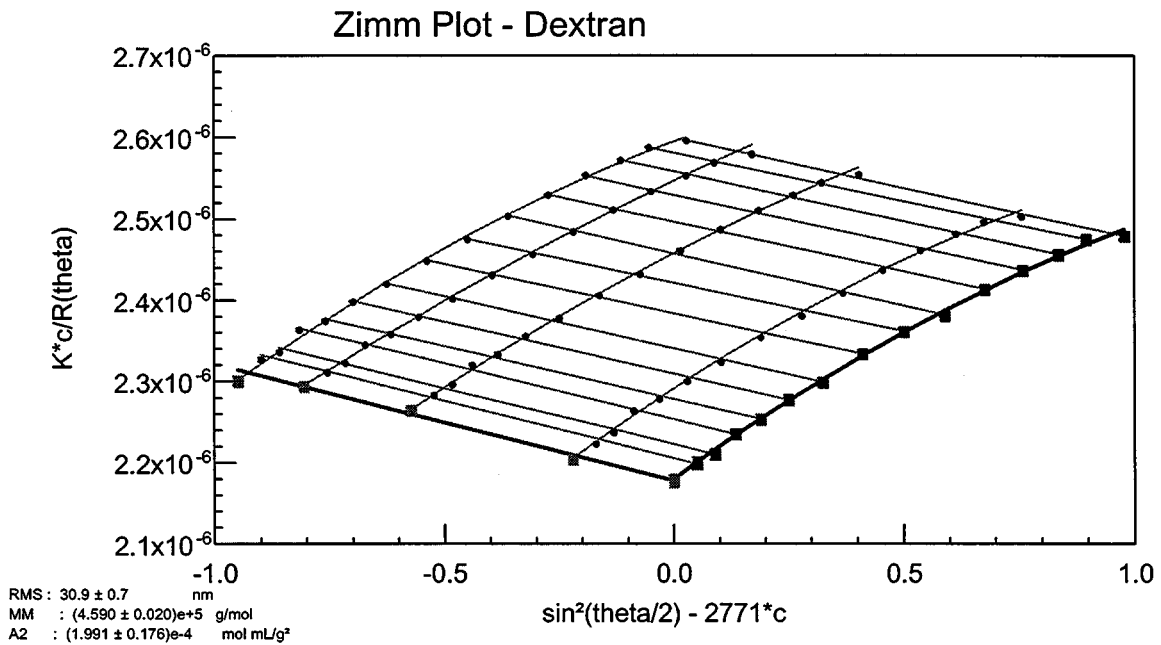


Figure 2.14 – Zimm plot for measurements taken from the multi-angle laser light scattering detector on a 500k dalton dextran.

this sample was 459,000 daltons (g/mole) and was determined as the reciprocal of the extrapolated value at zero angle and zero concentration. The measured value was close to the reported value for the dextran sample.

The size of the dextran molecules and the second virial coefficient are also determined from a Zimm plot. The root-mean-square (RMS) radius was determined from the slope of the fitted line through the extrapolated values of zero concentration. In this example, the fitted line was second order so the value of slope used was at zero angle. The measured RMS radius was 30.9 nm. The second virial coefficient was 1.991×10^{-4} mole mL/g² and was determined from the slope of the extrapolated values at zero angle. The second virial coefficient is a measure of the solvent-solute interaction.

The molar mass and the size of dextran samples were measured several times to develop the technique and to determine reproducibility. The results are summarized in Table 2.3. The average molar mass was 4.81×10^5 daltons and the average RMS radius was 33 nm. The molar mass values were within $\pm 5\%$ of the average and the RMS values were within $\pm 9\%$ of the average for these initial runs.

Table 2.3 – Molar mass and RMS radius for 500k dextran standard.

Run	1	2	3	4	5	6	7
Molar mass (10^5 daltons)	5.012	5.101	5.029	4.792	4.590	4.580	4.560
RMS radius (nm)	29.8	36.3	37.4	30.4	32.4	33.7	30.9

The solvent used for the dextran samples was an aqueous 100 ppm sodium azide solution and measurements were made at 25 °C. Refractive index of the solvent was 1.3325 and the refractive index increment (dn/dc) was 0.143 mL/g.

Weight-average molar mass and RMS radius for 200k polyacrylamide samples were measured and are presented in Table 2.4. The average value of the weight average molar mass was 806,000 daltons. The measured values were within 7% of the averaged value. The measured value for molar mass was about four times the value that was supplied with the sample. The sample was over ten years old and the procedure for determining the molar mass of the sample is unknown. Newer standards will be purchased and run to determine the accuracy of the measurements on polyacrylamides.

Table 2.4 – Molar mass and RMS radius for 200k polyacrylamide standard.

Run	1	2	3	4	5
Molar mass (10 ⁵ daltons)	8.37	7.78	8.36	8.32	7.47
RMS radius (nm)	111	102	107	109	100

The RMS radii of the 200k polyacrylamide samples are also presented in Table 2.4. The average value was 106 nm. The measured values are within 6% of the average. The solvent used for 200k polyacrylamide standard was 1 wt% KCl aqueous solution with 100 ppm sodium azide as a bactericide. The samples were measured at 25 °C. The refractive index of the solvent was 1.3336 and the refractive index increment (dn/dc) used was 0.190 mL/g. Measurements of the dn/dc value for polyacrylamide were inconsistent. The cause of the scatter in the values is being addressed.

Conclusions

1. Procedures to determine aggregate size distributions using equilibrium dialysis were developed and tested.
2. Aggregate growth with reaction time was observed for a polyacrylamide-chromide-acetate gelant using the equilibrium dialysis method.
3. Size distributions of spherical particle and polystyrene sulfonate polymer were determined using flow field-flow fractionation (FFFF).
4. Size distributions of polyacrylamide polymer solution were determined using FFFF and the results are consistent with the results determined using equilibrium dialysis. The results are also consistent with the values in literature.
5. Size distributions of a reacting polyacrylamide-chromium acetate gelant were determined using flow FFF. The aggregates become smaller in size with reaction time based on the systematic shifting of elution profiles to lower retention times. This trend is opposite to the results using equilibrium dialysis.
6. Procedures and techniques were developed for the determination of molar mass and root-mean-square radius using the multi-angle laser light scattering detector.

References

1. Benincasa, Maria Anna and Giddings, J. Calvin, "Separation and Molecular Weight Distribution of Anionic and Cationic water soluble polymers by Flow Field Fractionation," *Anal. Chem.*, **64** (1992) 790-798.
2. Giddings, J.C., Yang, F.J., Myers, M.N.: "Theoretical and Experimental Characterization of Flow Field-Flow Fractionation," *Analytical Chemistry*, **48** (1976) 1126-1132.

3. Giddings, J.C., Wahlund, Karl-Gustav, Winegarner, Helen S., and Caldwell, Karin D.: "Improved Flow Field-Flow Fractionation System Applied to Water-Soluble Polymers: Programming, Outlet Stream Splitting, and Flow Optimization," *Analytical Chemistry*, **58** (1986) 573-578.
4. Giddings, J.C.: "Hydrodynamic Relaxation and Sample Concentration in Field-Flow Fractionation Using Permeable Wall Elements," *Anal. Chem.*, **62** (1990) 2306-2312.
5. Hansen, Marcia, Giddings, J.C., and Li, Ping: "Advances in Frit-Inlet and Frit-Outlet Flow Field-Flow Fractionation," *J. Microcolumn Separations*, **10** (1997) 7-18.
6. Hecker, R, Fawell, P.D., Fefferson, A. and Farrow, J.B., "Flow Field-Flow Fractionation of High-Molecular-Mass Polyacrylamide," *Journal of Chromatography A*, **837** (1999) 139-151.
7. Huglin, M.B. (ed), *Light Scattering from Polymer Solutions*, Academic Press, London, (1972).
8. Kurata, M. and Tsunashima, Y.: "Viscosity-Molecular Weight Relationships and unperturbed Dimensions of linear Chain Molecules," *Polymer Handbook* J. Brandrup, E.H. Immergut, and E.A. Grulke (eds), John Wiley & Sons, New York City (1999) Section VII/1, 1-83
9. Lewis, Robert D., "An Experimental Study of Gel Aggregate Formation in a Polyacrylamide-Aluminium System," M.S. thesis, University of Kansas (1996).
10. McCool, C.S., Green D.W. and Willhite, G.P., "Permeability Reduction Mechanisms Involved in In Situ Gelation of a Polyacrylamide/Chromium(VI)/Thiourea System in Porous Media," *SPE Reservoir Engineering*, **6** (Feb. 1991) 77-83.
11. Meyers, M.N., Overview of Field-Flow Fractionation," *J. Micro Separations*, **9** (1997) 151-162.
12. Ying, H., Wu, G. and Chu, B., "Laser Light Scattering of Polyacrylamide in 1 M NaCl Aqueous Solution," *Macromolecules*, **29** (1996) 4646-4654.
13. Taylor, Kevin C. and Nasr-El-Din, Hisham A., "Acrylamide Copolymers: A Review of Methods for Determination of Concentration and Degree of Hydrolysis in Acrylamide Copolymers," *Journal of Petroleum Science and Engineering*, **12** (1994) 9-23.
14. Thielking, H and Kulicke, W-M., "Determination of the Structural Parameters of Aqueous Polymer Solutions in the Molecular, Partially Aggregated, and Particulate States by Means of FFFF/MALLS," *J. Microcolumn Separations*, **10**, (1998) 51-56.
15. Wyatt, P.J., "Light Scattering and the Absolute Characterization of Macromolecules," *Analytica Chimica Acta*, **272** (1993) 1-40.

Chapter 3

Effect of Added Acetate on the In Situ Gelation of the Polyacrylamide-Chromium(III) Acetate System

Graduate Research Assistants: Lingyun DU and Dilip Natarajan

Introduction

Chromium acetate-polyacrylamide systems have been used primarily to treat fracture systems, casing leaks and near wellbore regions in matrix rock where short gel times are acceptable. The relatively rapid chromium acetate-polyacrylamide reaction limits the application of this technology to near-wellbore treatment of matrix rock. Pre-gel aggregates form during the gelation reaction and some of these aggregates are filtered from the solution, thus building up high flow resistance and limiting the depth of penetration into the porous matrix. The rate of aggregate growth needs to be controlled to limit the rate of filtration for in-depth permeability modification in matrix rock.

Background

Syndansk [1990;1997], Syndansk and Argabright [1987] describe a family of chromium(III)-polyacrylamide gels ranging from highly flowing to rigid rubbery gels with a wide range of gel times. Burrafato and Lockhart [1989] and Burrafato et al. [1990] proposed that the chromium uptake from chromium-carboxylate complexes is a ligand exchange reaction in which a carboxyl group on the polyacrylamide displaces ligands (i.e. acetate). Crosslinking occurs when a second polyacrylamide molecule reacts with the attached chromium. The reaction chemistry between Cr(III) and polyacrylamide is complex as the structure of chromium and the attached ligands vary with pH and temperature. The chromium uptake and crosslinking reactions are described in Eq.3.1 and Eq.3.2. The symbol OAc^- indicates an acetate ion and the symbol P-CO_2^- indicates a reactive carboxyl group on a polymer molecule. Acetate ion is a product of these reactions which suggests that addition of acetate to the gel solution would limit chromium uptake and crosslinking or would reduce the rates of these reactions.

Uptake Reaction



Crosslinking Reaction



Green et al. [1993] studied the effect of various ligands like acetate, nitrate, chloride etc. and their concentrations as free ligands in solution on the gel times of the polyacrylamide - chromium (III) system. These studies showed that the use of chromium acetate and the presence of free acetate in solution could delay gelation significantly at 25°C.

Bottle tests and displacement experiments were conducted by Natarajan et al. [1998] to determine the effect of added acetate on performance of the polyacrylamide-chromium(III) gel system. Increased concentrations of sodium acetate were shown to delay gelation. Displacement

experiments in sandpacks (1ft to 6 ft long) showed that increased acetate concentrations delayed the development of flow resistance during gelant injection in porous media. Development of flow resistance in the sandpacks was significantly faster than the gel times observed in bottle tests.

The objective of this work was to determine if insitu gelation is delayed using a gel system containing added acetate. The performance of a polyacrylamide-chromium acetate system was tested by flow experiments in a 40-foot long sandpack. The concentration of added acetate in the gel system was initially selected to give a gel time of approximately 3 months, much longer than the time for placement in the sandpack. However, the flow experiment was conducted with a different polymer lot since the original lot was exhausted. It was subsequently determined that gelants prepared with the new lot did not gel as readily and the system injected in the sandpack did not gel in a bottle within two years.

Experimental Details

A displacement experiment was designed to study the injection characteristics of the gel system in a 40-ft sandpack. A schematic of the experimental setup is shown in Figure 3.1. The sandpack holder was a 1.475 inch ID PVC tube fitted with ports for measurement of pressure. The ports divided the sandpack into six sections of about 6.75 ft long. Silica sand (Wedron Silica Company; 144 mesh) was acid washed, rinsed in distilled water, dried and packed. Screens were placed at the inlet and outlet and in the pressure port fittings to avoid sand washout. Pressure ports were connected to transducers to measure the differential pressure across sections. Pressure data were collected with a computer-based data acquisition system.

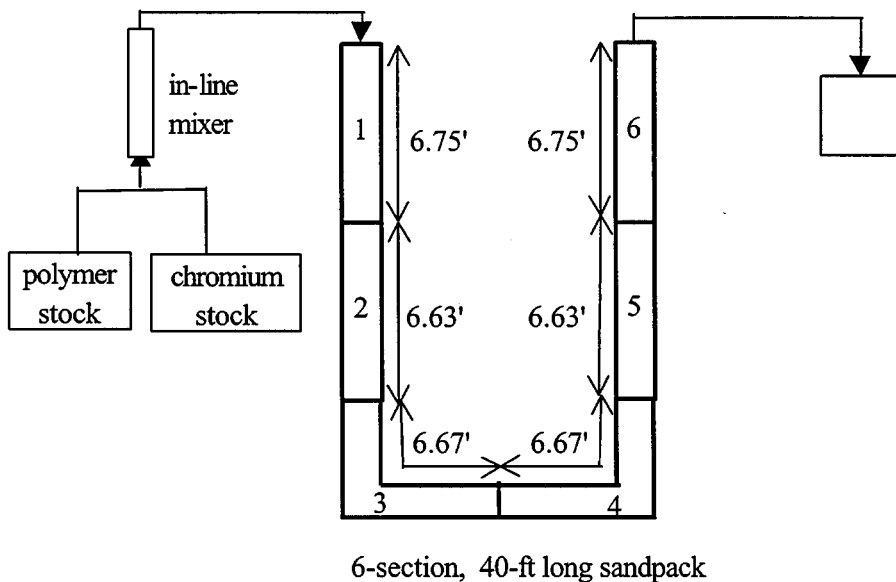


Figure 3.1 – Schematic of apparatus for flow experiments.

The sandpack was saturated with water and a tracer test was conducted to determine the pore volume of the sandpack. The pore volume was 4910 mL. Water was injected through the pack to determine the permeability of the entire length and the individual sections. The permeabilities are listed in Table 3.1.

Table 3.1 – Permeabilities for the 40-ft sandpack in millidarcies.

Section 1	Section 2	Section 3	Section 4	Section 5	Section 6	Overall
3883	4503	4151	4363	4421	3520	4279

The pH of the sandpack was stabilized at the pH value of the gelant (5.0 ± 0.1) before injection of gelant. This was accomplished by the injection of a buffer solution containing sodium acetate and acetic acid. The concentration of acetate in the buffer solution was equal to the concentration of acetate in the gelant.

A polymer stock solution containing Alcoflood 935 (Ciba; batch #7158V) polyacrylamide and sodium acetate was prepared and allowed to mix for one day before use. The pH of the polymer solution was adjusted with acetic acid to a value such that the pH of the gelant would be 5.0 ± 0.1 . The amount of acetic acid was measured to determine the total amount of acetate in the gelant. A stock chromium acetate solution was prepared from a 50% solution of chromium acetate obtained from McGean Rocho. The stock chromium acetate solution was prepared just before use. Mixing of the stock polymer and chromium acetate solutions at a weight ratio of 3:1 produced a gel solution containing 5000 ppm polyacrylamide, 109 ppm Cr(III) and 0.25 mol/L sodium acetate. The pH of the gelant was 5.0 ± 0.1 .

The stock polymer and chromium acetate solutions were mixed inline and injected through the sandpack at a total flow rate of 0.6 mL/min. Pressure drops were measured during gel injection and effluent samples were collected at regular intervals using an automatic sample collector. Gel injection was stopped after about 1.2 PV of injection and the experiment was shut in for about 18 months. Manually mixed gel samples and samples from the in-line mixer were collected to observe the bulk gel times. All procedures were conducted at room temperature.

Post-treatment flow experiments were conducted after the 18 month shut-in period to determine the performance of the gel system. A polymer solution containing 5000 ppm polyacrylamide (Alcoflood 935, Batch #7158 V), and 0.22 mol/L sodium acetate was injected into the sandpack. The flow rate was initially 0.6 mL/min but was reduced to 0.3 mL/min when the injection pressure became excessive. The pH of the polymer solution was adjusted to 5.0 and the viscosity was about 20 cp at a shear rate of 45.0 sec^{-1} .

Results and Discussion

Gelant was mixed inline and injected into the 40-foot long sandpack for 160 hours. Approximately 1.2 pore volumes of gelant were injected. Pressure data collected during the injection process were converted to apparent viscosities and are shown in Figure 3.2 as a function of pore volumes injected. Apparent viscosity is a measure of the average flow resistance

in the sandpack over which the pressure differential was measured and is calculated by Darcy's law using the initial permeability of the interval. Progression of the more viscous gelant as it displaces the less-viscous brine from each of the sections is shown in Figure 3.2. The apparent viscosity of the gelant was about 35 cp. Development of higher flow resistances was not observed during the injection of 1.2 PV of gelant indicating no insitu gelation occurred during the injection process. The high acetate concentration in the gelant inhibited insitu gelation.

The sandpack was shut-in for 18 months. Samples of the gelant that were manually mixed, collected from the in-line mixer prior to injection and collected from the core effluent showed no increase in viscosity for two years. It was suspected that insitu gelation did not occur since the bulk samples had not gelled within the 18 month period. It was decided to displace the gelant from the pack with polymer solution in order to have favorable mobility control and minimize mixing between the injected solution and the resident gelant. This injection method was conducted to allow for easier interpretation of the pressure data and chemical analyses of the effluent.

Pressure data taken during the injection of polymer solution are presented in Figure 3.3 as apparent viscosities as a function of core length. Pressure data for Sections 2 and 3 were combined because the common pressure port between these sections was plugged and not sensing the pressure correctly. The flow resistance in the sandpack, as shown by the apparent viscosity profiles in Figure 3.3, ranged between 20 and 40 cp during the injection of the first 0.15 pore volumes of polymer. This range is typical for the flow of polymer in these packs. Development of increased flow resistance was observed only in Section 4 and occurred between 0.1 and 0.39 pore volumes injected. Injection was stopped at 0.39 pore volumes injected due to high injection pressure. At that time, the front of the injected polymer solution progressed part way into Section 3, assuming plug flow. (Each section contained about 0.17 pore volumes of fluid.) The development of increased flow resistance in Section 4 was unexpected and the cause was unknown.

Viscosity of the effluent during polymer injection was measured and ranged between 8 to 12 cp at a shear rate of 45 sec^{-1} . Viscosity of a bulk sample of the injected gelant after 18 months was 20 cp at shear rate of 45 sec^{-1} . The cause of the decrease in viscosity of the gelant that was aged in the sandpack is unknown. The pH of the effluent was around 5.10, which was close to the pH of the fluid originally injected. The effluent was a pinkish color which was in contrast to the green color of the gelant samples that had been aged for 18 months. The cause of the color change is being addressed. Analysis of the chromium concentration in the effluent samples has not been conducted to date.

Summary and Future Plans

This work demonstrated that a polyacrylamide-chromium(III) gel system can be propagated a distance of 40 feet over a time period of 160 hours without the development of increased flow resistance. Addition of added acetate to the gel system inhibited the insitu gelation process to the point where additional retention of polymer and/or polymer aggregates caused by the gelation process did not occur. The gelant did not form a continuous gel within the pores of the sandpack during an 18-month shut-in period. This was expected since samples of the injected gelant did

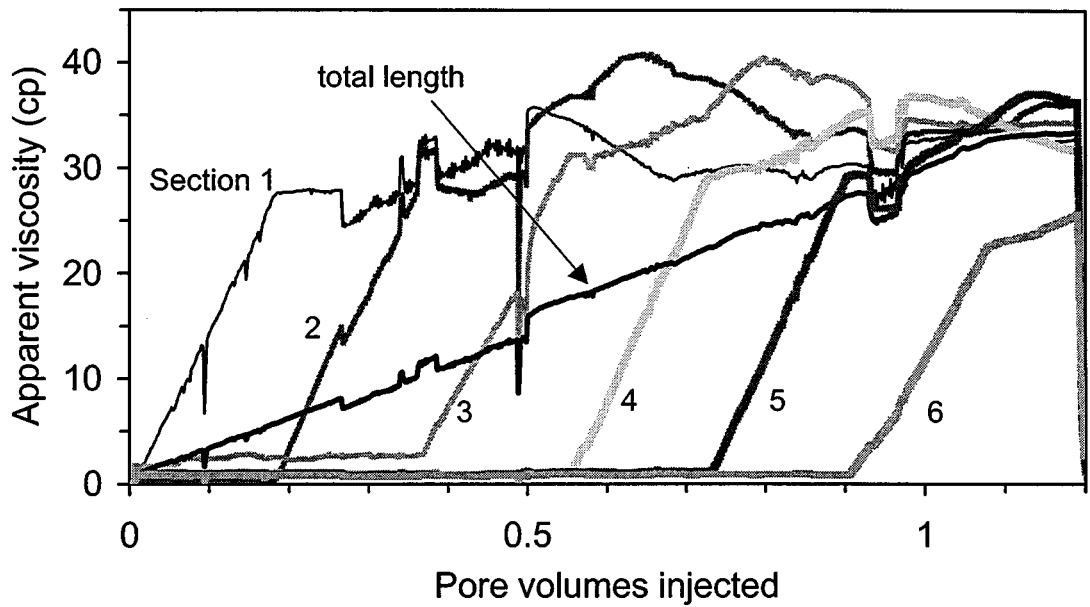


Figure 3.2 – Flow resistance in sandpack during injection of gelant.

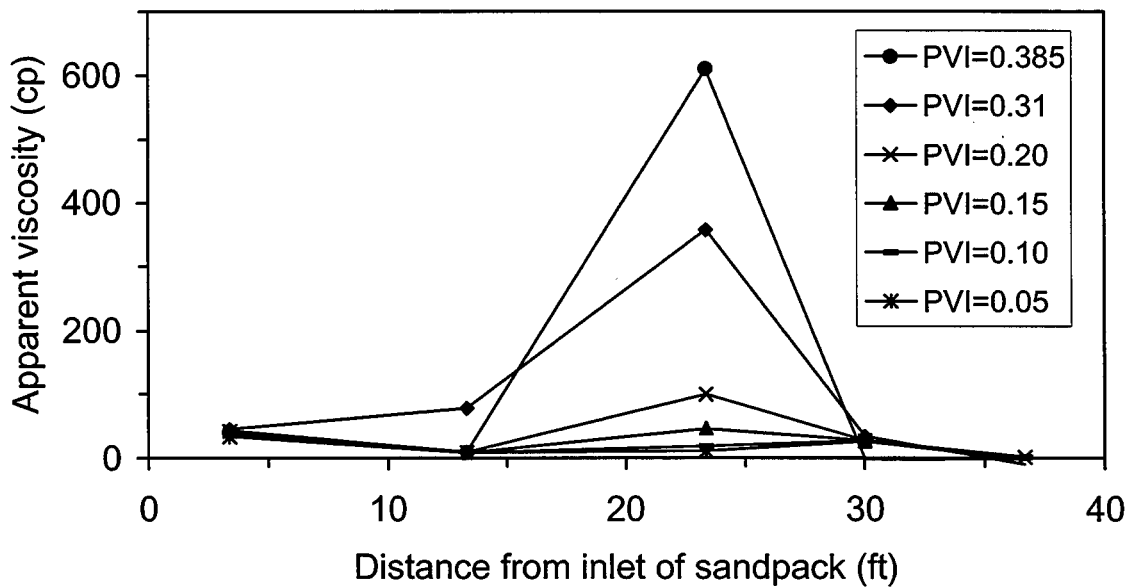


Figure 3.3 – Flow resistance profiles in sandpack during injection of brine.

not gel. However, high flow resistance developed in one section of the sandpack during displacement of the gelant by polymer after the shut-in period. It was unclear why high flow resistance developed in only one zone of the sandpack

The 40-foot long sandpack will be examined to determine the extent of the zone where high flow resistance occurred and the cause of the high flow resistance. Analysis on the core effluent will be conducted to determine chromium concentration and the cause of the pink color.

Flow experiments will be designed and conducted in sandpacks of various lengths to determine if the polyacrylamide-chromium(III) system can be formulated with added acetate to allow in-depth placement. That is, the system should be able to be injected a sufficient distance before increased flow resistance develops.

References

1. Burrafato, G. and Lockhart, T.P., "A New, Mild Chemical Method for the Degelation of Cr -Polyacrylamide Gels," Society of Petroleum Engineers paper No. 19354 (submitted May 1989).
2. Burrafato, G. Albonico, P., Bucci, S. and Lockhart, T.P., "Ligand -Exchange Chemistry of Cr+3-Polyacrylamide Gels," *Makromolec. Chem., Macromol, Symposium*, **39** (1990) 137-141.
3. Green, D.W., Willhite, G. P., McCool, C. S. and McGuire, M., "Improving Reservoir Conformance Using Gelled Polymer Systems," Annual report for the period September 25 1992 to September 24 1993, DOE contract No. DE-AC22-92BC14881, Report No. DOE/BC/14881-5, Chapter 5, The University of Kansas.
4. Natarajan, D., McCool, C.S., Green, D.W. and Willhite, G.P., "Control of In-Situ Gelation Time for HPAAM-Chromium Acetate Systems," paper SPE 39696 presented at the 1998 SPE/DOE Improved Oil Recovery Symposium, Tulsa, OK (19-22 April).
5. Sydansk, R.D. and Argabright, P.A., "Conformance Improvement in a Subterranean Hydrocarbon - Bearing Formation using a Polymer Gel," U.S Patent 4,683,949 (Aug. 4, 1987).
6. Sydansk, R. D., "A Newly Developed Chromium(III) Gel Technology," *SPE*, (August 1990) 346-352.
7. Sydansk, R. D., "pH Dependent Process for Retarding the Gelation rate of a Polymer Gel Utilized to Reduce Permeability in or Near a Subterranean Hydrocarbon-Bearing Formation," U.S. Patent 5,609,208 (March. 11, 1997).

Chapter 4

Chromium (III) Transport in Carbonate Rock

Graduate Research Assistant: Hong Jin

Introduction

The chromium(III)-polyacrylamide system is a commonly used gel system in permeability modification treatments in oil reservoirs. During the placement of the gel system in carbonate reservoir rock, the transport of chromium(III) is often limited by precipitation. Precipitation occurs due to the elevated pH environment that is encountered in carbonate rocks as the result of the dissolution of carbonate minerals.

Several investigators have studied the application of chromium-crosslinked gel systems to carbonate reservoirs. McCool et al. [2000] studied the interaction between dolomite cores and a xanthan-Cr (III) gel system, Seright [1992] studied the propagation of chromium acetate and chromium chloride in Indiana limestone cores, and Stavland et al. [1993] studied chromium retention in Berea and Brent sandstone cores. These studies concluded that precipitation was the primary mechanism of chromium retention in the cores and the precipitation was caused by the dissolution of carbonate minerals that increased the pH of the injected solution.

This research is a continuation of work conducted by Zou who studied the interactions between KCl brine solutions and dolomite rock [Zou et al.; 2000a] and the precipitation of chromium from chromium acetate solutions [Zou et al.; 2000b]. KCl solutions at pH values between 2.6 and 12.8 and at selected flow rates were injected through dolomite rock to study the effects of the injected pH value on dolomite dissolution and pH changes in the flowing solution. Experiments at different flow rates established conditions in which dolomite dissolution achieved equilibrium in the rock and indicated that an equilibrium state exists for most field conditions. The pH in the rock at equilibrium was almost constant at a value of approximately 9.8 when the brine was injected at pH values that ranged from 4 to 10. Addition of calcium and magnesium ions in the injected brine suppressed dolomite dissolution and affected the effluent pH from the dolomite rock moderately. An equilibrium geochemical model accurately predicted the pH and component concentrations that result from the interactions between brine and dolomite rock.

Precipitation of chromium from chromium acetate solutions was studied as a function of pH, temperature, salinity, and acetate concentration [Zou et al.; 2000b]. Experiments were conducted with bulk solutions in which the pH of the solution was adjusted and then controlled at a constant value by the addition of a NaOH solution. Chromium did not precipitate immediately in most cases. An induction period occurred after which the chromium precipitated. Increase in pH, temperature, and salinity decreased the induction period and increased the precipitation rate. Increase in acetate concentration moderately reduced the chromium precipitation rate over the range studied.

An empirical kinetic model was developed by Zou et al. [2000b] to describe chromium precipitation as a function of chromium concentration, initial pH, and acetate concentration at

25°C. The model simulates the induction period and the chromium concentration in batch scale experiments (at constant pH) as a function of time. The model predicted the pH and chromium concentration as a function of time for the experiments where ground dolomite was added to the chromium acetate solution.

The objectives of this work are to determine the characteristics of chromium (III) transport through dolomite rock and to determine applicability of the models developed by Zou et al [2000b] to describe chromium retention in flow experiments. This chapter presents the progress made to date to achieve these objectives.

Experiment

Flow Experiments. Two types of flow experiments were conducted to study the transport of chromium (III) through dolomite rock: constant-rate experiments and shut-in experiments. In the constant-rate experiments, a chromium acetate solution was continuously flowed through a dolomite core at various rates. In the shut-in experiments, a chromium acetate solution was quickly injected into the dolomite core and the core was shut-in for a selected period of time. Chromium solution was then quickly injected again to displace the solution that was in the core during the shut-in period.

A schematic of the experimental set-up for the flow experiments is shown in Figure 4.1. Two ConstaMetric 2000 pumps were used to inject solutions under constant rate. Water, brine, chromium acetate solutions and a tracer solution were injected. A four-way valve between the pumps and the core facilitated the change of fluid that was delivered to the dolomite core. A six-way valve allowed for the injected fluid to bypass the core. Small diameter tubing (0.01 inch ID) was substituted during the experimental work to minimize dead volumes. A pressure transducer measured the differential pressure along the core. An in-line ISCO spectrophotometer and an in-line pH meter were connected to the exit of the core. The spectrophotometer provided data to determine effluent chromium and tracer concentrations. An automatic fraction collector was used collect effluent samples. Chromium concentrations in the effluent fractions were determined by atomic absorption spectrophotometry (AAS). A Camile TG system was used for data acquisition and valve control.

Chromium Analyses Sample treatment was crucial for the analysis of chromium concentration. Effluent fractions from the flow experiments were diluted and acidified to a pH of approximately 2 with 1% nitric acid immediately after collection to eliminate additional precipitation. Chromium concentrations were then determined for the fractions/samples with a Perkin-Elmer Analyst 300 using standard methods.

Chromium concentrations were also determined using an inline ISCO V4 spectrophotometer during flow experiments. Chromium(III) was detected at a wavelength of 414nm. Interference from other chemicals at this wavelength was minimized as shown by the absorbance-wavelength scans in Figure 4.2.

Chemicals. Chromium acetate was obtained from Alpha Products (Danvers, MA) in the form of a dark green powder with the formula of $\text{Cr}(\text{OOCCH}_3)_3 \cdot \text{H}_2\text{O}$. Solutions were prepared by dissolving chromium acetate in water and KCl brine solutions. Chromium solutions were aged

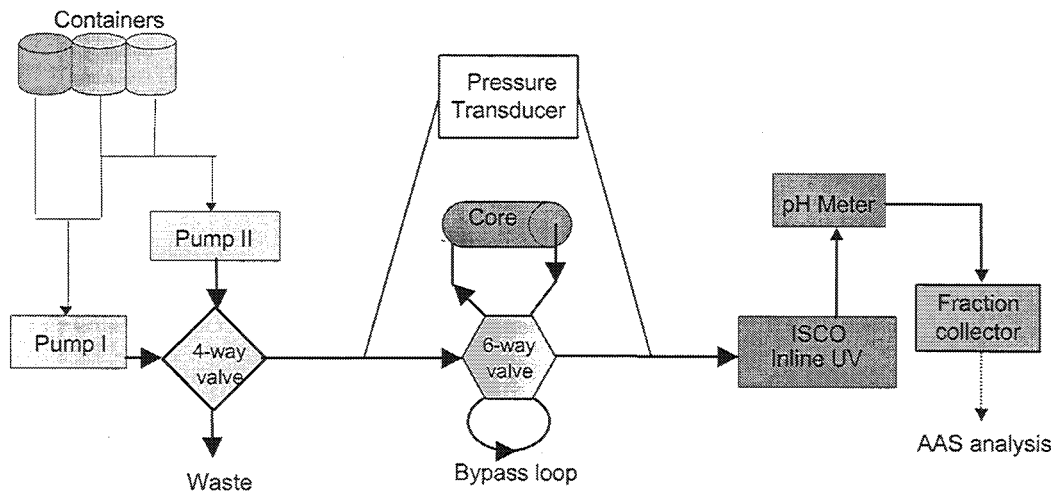


Figure 4.1 – Schematic of equipment for flow experiments.

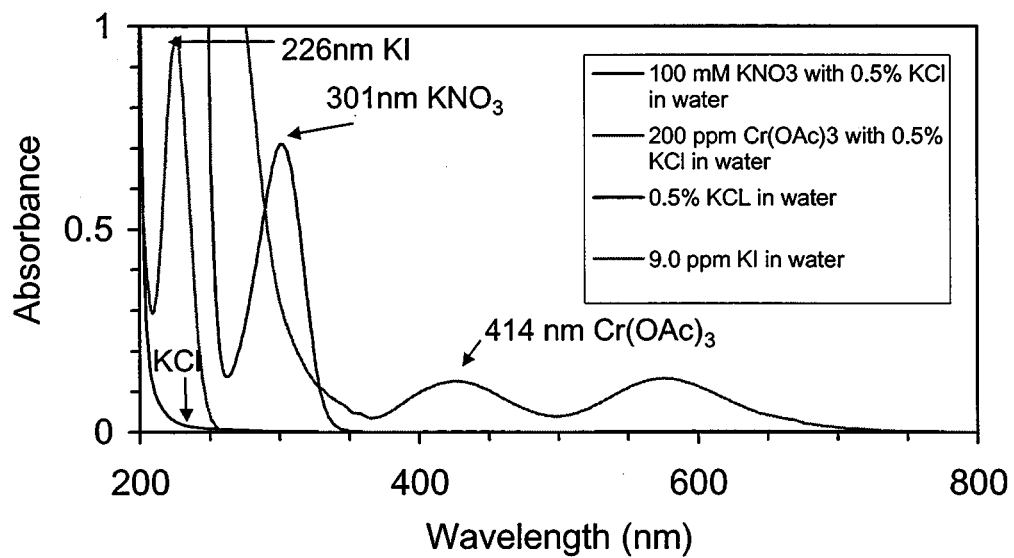


Figure 4.2 – Absorbance scans of solutions used in study.

for seven days before use. The concentration of chromium was 200 ppm by weight. KCl was obtained from Fisher Scientific. High-grade laboratory water (resistivity > 18 megohm-cm) was used to prepare all solutions.

Two tracers were used to determine the flow characteristics of the dolomite cores. It was assumed that the tracers, potassium iodide and potassium nitrate, would not be retained in the cores. The potassium iodide (40 ppm) solution and the potassium nitrate (10,100 ppm KNO₃; 1% KCl) solution were detected in the core effluent by the ISCO V4 spectrophotometer at wavelengths of 226nm and 301nm, respectively.

Dolomite cores. The rock material studied was Baker dolomite (Millersville, OH). Baker dolomite is relatively pure, containing mole percentages of calcium carbonate and magnesium carbonate of 57 and 43, respectively [Meister; 1978]. Two cores were drilled in cylindrical shape, washed with water, and dried in the oven at about 100 °C. Endplates were attached to the cores and then coated with epoxy. Core names and properties are listed in Table 4.1.

Table 4.1 - Core Properties.

	Bin #4	Hong #3
length (cm)	7.8	4.8
diameter (cm)	1.8	1.9
porosity (%)	22	21
pore volume (mL)	4.41	2.85
permeability (md)	30	25

Results and Discussion

Flow Experiments at Constant Flow Rate. The following runs in the dolomite core Bin #4 documented the transport characteristics of chromium (III) during flow through dolomite.

Runs were conducted by injecting a series of solutions, each for a time period of two hours and at a flow rate of 0.19 mL/min. A tracer (40 ppm KI in 0.5 % KCl brine) was injected first followed by the injection of 0.5 % KCl brine. This sequence was repeated five times to check the reproducibility of the tracer response. A chromium acetate solution (200 ppm chromium) was then injected followed by 0.5 % KCl brine. This sequence was also repeated five times.

Normalized concentrations in the effluent for the tracer (one run) and chromium are presented in Figure 4.3 as a function of time. Time zero represents the start of the injection of tracer and the five chromium acetate solutions. Brine was injected between 120 and 240 minutes for the six runs that are shown. The pore volume of Bin #4 was 4.41 mL and the total volume between the inlet switching valve and the UV detector was 5.1 mL. These volumes represent residence times of 23 minutes in the core and 27 minutes in the total volume of the system.

Chromium concentrations determined by inline UV detector are presented as solid lines in Figure 4.3. Chromium concentrations were determined by AAS for one run and are presented as

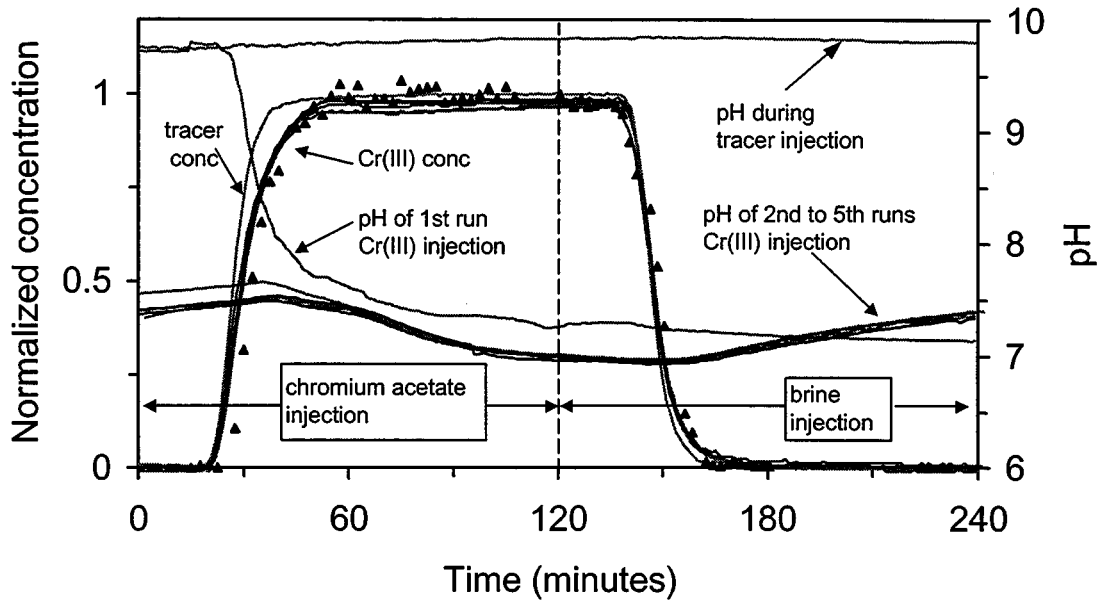


Figure 4.3 – Normalized chromium concentration and pH in the effluent for alternate injection of chromium acetate solution (200ppm chromium; 1.0% KCl) and KCl brine; Core Bin#4.

triangles. Chromium was retained in the core in each of the runs as shown by the differences between the concentrations of tracer and chromium. Chromium retention occurred at the front end of the flowing chromium solution as well as during the plateau region between 50 and 140 minutes. The results of a material balance on chromium for the first run are given in Table 4.2. The amount of chromium retained per gram of rock is not large which is due, in part, to the short residence time of 22 minutes. Additional chromium was retained in the subsequent runs and it appears that this retention would occur indefinitely. These observations indicated that adsorption was not the dominate retention mechanism.

Table 4.2 - Material Balance on Chromium for Runs in Figure 4.3.

Analysis Method	Amount Injected (μg)	Amount Recovered (μg)	Amount Retained (μg)	Amount Retained (μg/g rock)
ISCO UV	4780	4630	150	3.54
AA	4760	4650	110	2.60

Effluent pH values measured during this series of runs are also shown in Figure 4.3. The pH remained at 9.8 during the injection of tracer and the subsequent brine injection. 9.8 is the

equilibrium pH value that is obtained due to dolomite dissolution in unbuffered KCl brines with initial pH values between 4 and 10 [Zou et al.; 2000a]. During the injection of the first chromium acetate solution, the pH value of the effluent decreased from 9.8 to approximately 7 as chromium was detected in the effluent. Thereafter, the pH value remained between 6.9 and 7.5 during the injection of both chromium solution and brine. The displacement of several hundred pore volumes of brine was required during post-flooding before the effluent pH attained the value of 9.8. The slow recovery of pH after the core was contacted with chromium acetate is addressed later.

A second experimental set was conducted as a series of fluid displacements in core Hong#3. The objective of the runs was to determine the effects of flow rate and salt concentration on the retention of chromium during flow of chromium acetate solutions through dolomite. The experimental set-up was the same as the previous experiment except the dead volumes between the inlet switching valve and the core and between the core and the UV detector (0.03 mL) were reduced to a small percentage of the core's pore volume (2.85 mL).

A potassium nitrate tracer was first injected to determine the effluent concentration profile of a non-retained chemical. The tracer test was conducted at 1.0 mL/min. Chromium acetate solutions (200 ppm chromium) prepared in 0.5% and 1.0% KCl brines were injected at rates of 0.02 mL/min and either 0.10 mL/min or 1.00 mL/min. In between the injections of chromium acetate solutions, KCl brine was injected until the effluent pH of 9.8 was attained (except 0.5% KCl at 0.02 mL/min). Several hundred pore volumes of brine were required.

Normalized chromium concentrations in the effluent during the injection of chromium acetate solutions (200 ppm chromium) in 0.5% KCl are shown in Figure 4.4 as a function of pore volumes injected. The runs were conducted at 0.10 and 0.02 mL/min which correspond to residence times of 28 and 142 minutes, respectively. The profile of the normalized tracer concentration is also presented in the figure. The difference between the tracer and chromium concentration curves represents the amount of chromium that was retained. Chromium was retained at both flow rates with greater retention at the lower flow rate (or longer residence time). Similar results are shown in Figure 4.5 for the injection of chromium acetate (200 ppm chromium) solutions in 1.0% KCl at injection rates of 1.0 and 0.02 mL/min.

The profiles of the chromium concentrations in Figures 4.4 and 4.5 were approaching steady-state values after three-to-four pore volumes injected. The "steady-state" values at the lowest injection rate (0.02 mL/min), or the longest residence time, were less than the values for the higher injection rates, or shorter residence time. This observation indicated that the mechanism for chromium retention was a rate dependent process.

The effect of salt concentration on the retention of chromium is shown in Figure 4.6 where the effluent chromium profiles for chromium acetate solutions prepared in 0.5 and 1.0% KCl are plotted for the same injection rate of 0.02 mL/min. The tracer curve is also shown. More chromium retention was observed for the solution prepared in 1.0% KCl. This trend appears consistent with work by Zou et al. [2000b] on the precipitation of chromium from chromium

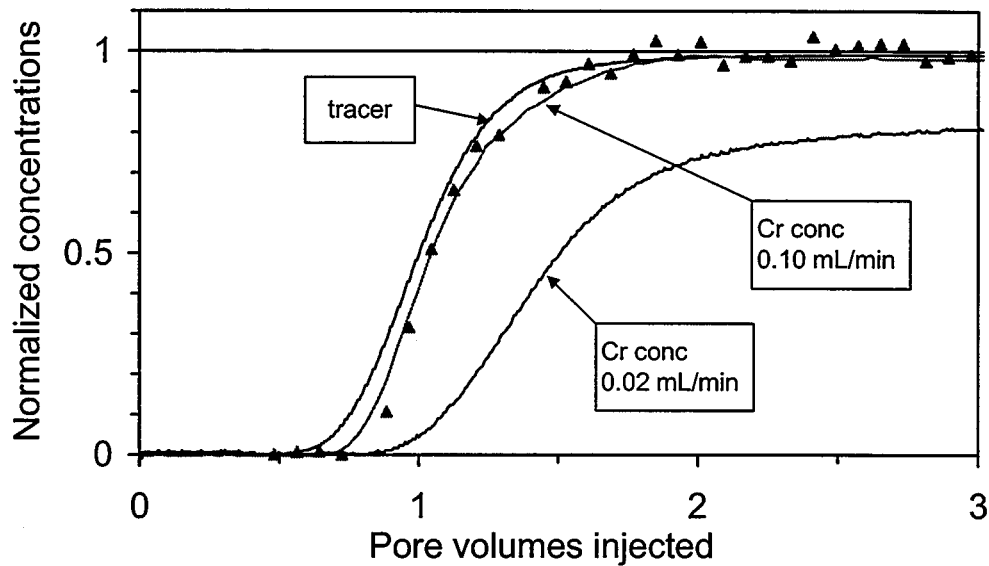


Figure 4.4 – Effect of flow rate on the normalized chromium concentration in the effluent during the injection of chromium acetate solutions (200ppm chromium; 0.5% KCl); Core Hong#3.

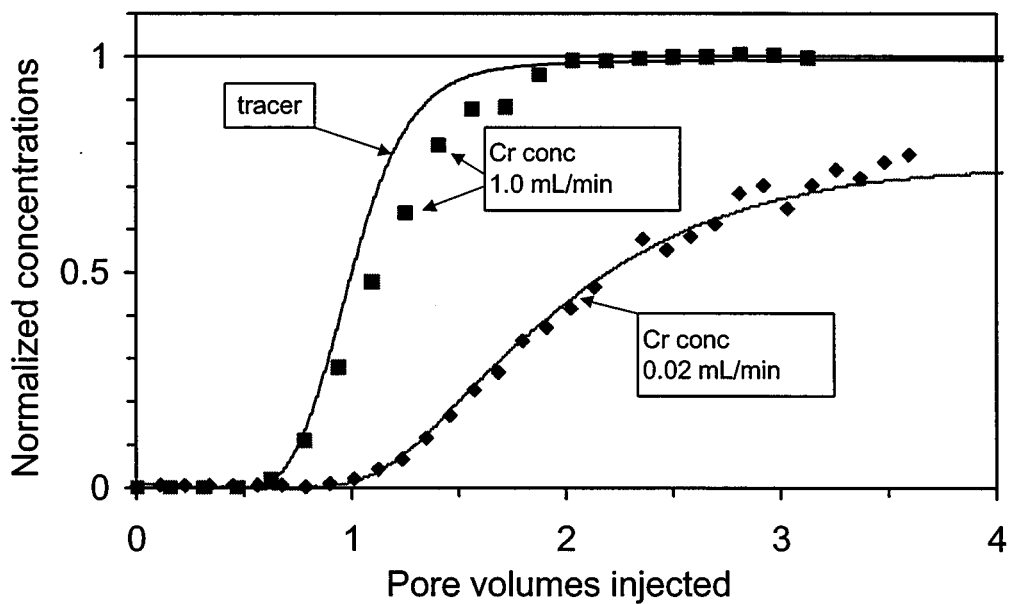


Figure 4.5 - Effect of flow rate on the normalized chromium concentration in the effluent during the injection of chromium acetate solutions (200ppm chromium; 1.0% KCl); Core Hong#3.

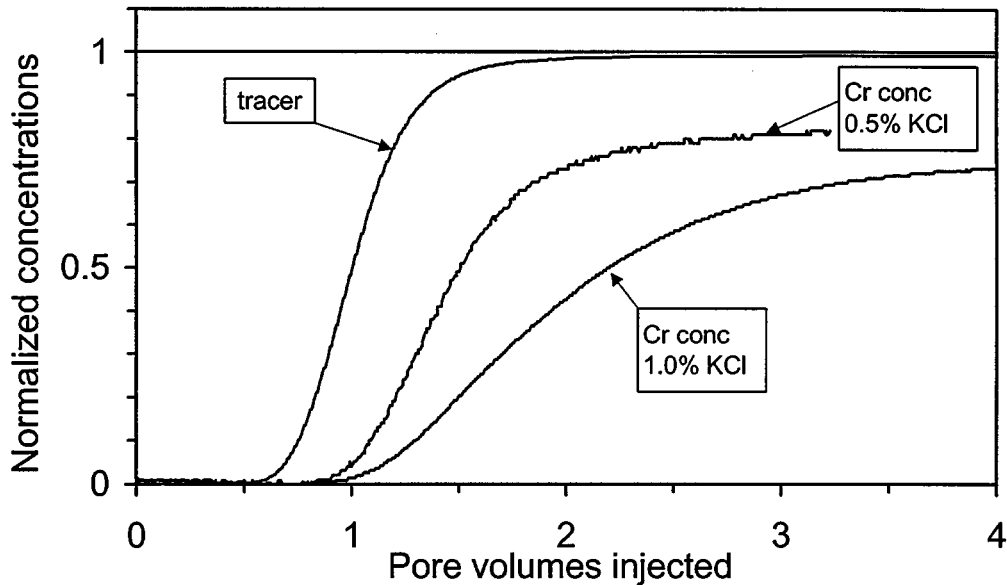


Figure 4.6 - Effect of KCl concentration on the normalized chromium concentration in the effluent during the injection of chromium acetate solutions (200ppm chromium); Core Hong#3.

acetate solutions. They observed faster precipitation rates with increased KCl concentrations. However, there were small differences in the effluent pH of the two runs shown in Figure 4.6 that would also affect the precipitation of chromium.

Flow Experiments with Shut-In Procedure. The core size and the performance of the pumps limited the length of time the injected fluid resides in the core during constant flow rate displacements (residence time). Flow experiments were designed with a shut-in period to achieve longer time periods for contact between the chromium acetate solution and the dolomite core. A chromium acetate solution (200 ppm chromium; 1.0% KCl) was injected quickly (1.0 mL/min; residence time of 2.8 minutes) through dolomite core Hong#3 for 30 minutes. Minimal amounts of chromium are retained in the core during the injection time. The core was then shut-in for a selected time period. This process was repeated for several shut-in time periods.

Normalized chromium concentrations in the effluent after a shut-in period are shown in Figure 4.7 for three shut-in periods of 24, 36 and 48 hours. Chromium concentrations during the first half pore volume injected represent the amount of chromium that remains in solution in the core during the shut-in period. About 80% of the chromium was retained in the core for a 24-hour shut-in period. Additional chromium was retained for longer shut-in times.

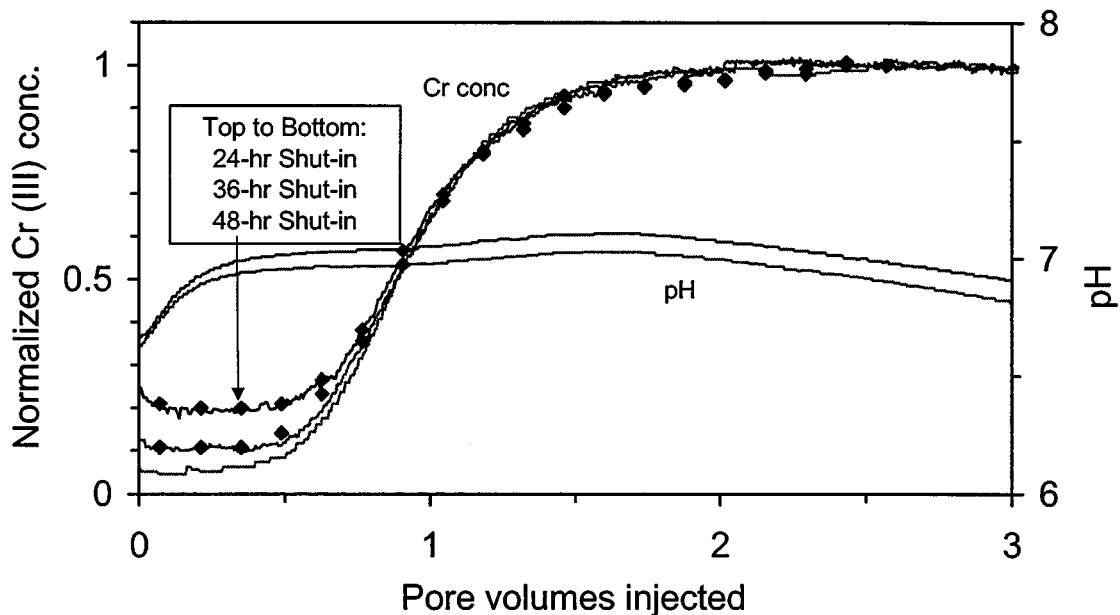


Figure 4.7 - Effect of shut-in time on the normalized chromium concentration in the effluent during the injection of chromium acetate solutions (200ppm chromium; 1.0% KCl); Core Hong#3.

The effluent pH values for two of the runs are also shown in the Figure 4.7. Values of pH for all the runs were between 6.5 and 7.3 for the fluids that were contained in the core during the shut-in periods. The shut-in times ranged from 0.5 to 48 hours. The pH values decreased for longer shut-in times.

Chromium concentrations that were measured in the chromium acetate solutions were plotted as a function of the shut-in time in Figure 4.8. Also plotted in the figure are the effluent chromium concentrations (at the steady-state condition; ~3PVI) from the constant rate experiments as a function of residence time. A trend line was regressed through the data. These data demonstrate the kinetic process of chromium retention in dolomite rock. It also appears that the data from the shut-in type of experiments were analogous to data obtained from constant rate injections. Plans for conducting runs at constant flow rate with longer residence times (to compare to the longer shut-in times) will test this analogy.

The chromium retention data were compared to a kinetic model developed by Zou et al [2000b]. The model described the precipitation of chromium from bulk chromium acetate solutions in experiments where the pH of the solution was adjusted and controlled at constant pH values by the addition of KOH solutions. It was observed in those experiments that chromium precipitated after an induction period and that the length of the induction period and the precipitation rate were functions of pH. Model results for a run at a pH value of 7 are shown in Figure 4.8. (The pH values of the solutions exiting the core after precipitation ranged from 6.5 to 7.3.) No

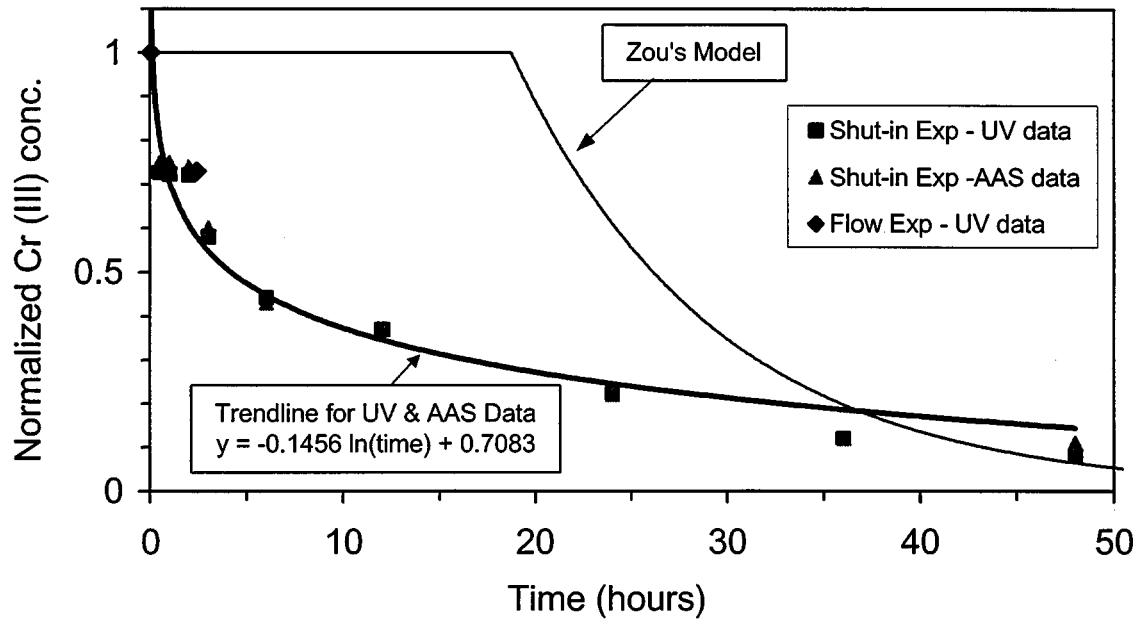


Figure 4.8 – Normalized chromium concentrations as functions of shut-in time, residence time and reaction time.

induction period was observed in the cores compared to an induction period of approximately 19 hours in the model. The model does not predict accurately the precipitation behavior in the dolomite cores. Chromium precipitated much faster in the cores than in experiments where the pH of the solutions was controlled by addition of base.

Recovery of Equilibrium pH after Injection of Chromium Acetate. It was observed during flow experiments that after the cores were contacted with chromium acetate solutions, the injection of several hundred pore volumes of brine was required before the effluent pH would attain the equilibrium value of 9.8. Dolomite dissolution in unbuffered brines with pH values between 4 and 10 causes the pH of the brine to increase to 9.8 [Zou et al.; 2000a]. The slow recovery of the effluent pH during the injection of KCl brine in Core Hong#3 is shown in Figure 4.9. Brine was injected at three flow rates. The data were comparable when plotted as a function of pore volumes injected. The slow recovery of pH was only dependent on the amount of brine that was injected, not the injection rate, which indicated that the mechanism responsible for the pH recovery was an equilibrium process at the flow rates tested.

Effect of Acetate on the pH in Dolomite Cores. The effluent pH during the injection of chromium acetate solutions in the dolomite cores generally ranged around a value of 7. A question arose to if this value of pH was result of the buffering capacity of the acetate ion. A series of runs were conducted to determine the effect acetate had on the pH of solutions in dolomite cores. A solution containing 0.0114 M sodium acetate and 1% KCl was prepared and the pH was adjusted to 5. This solution contains the same amount of acetate and KCl and was at

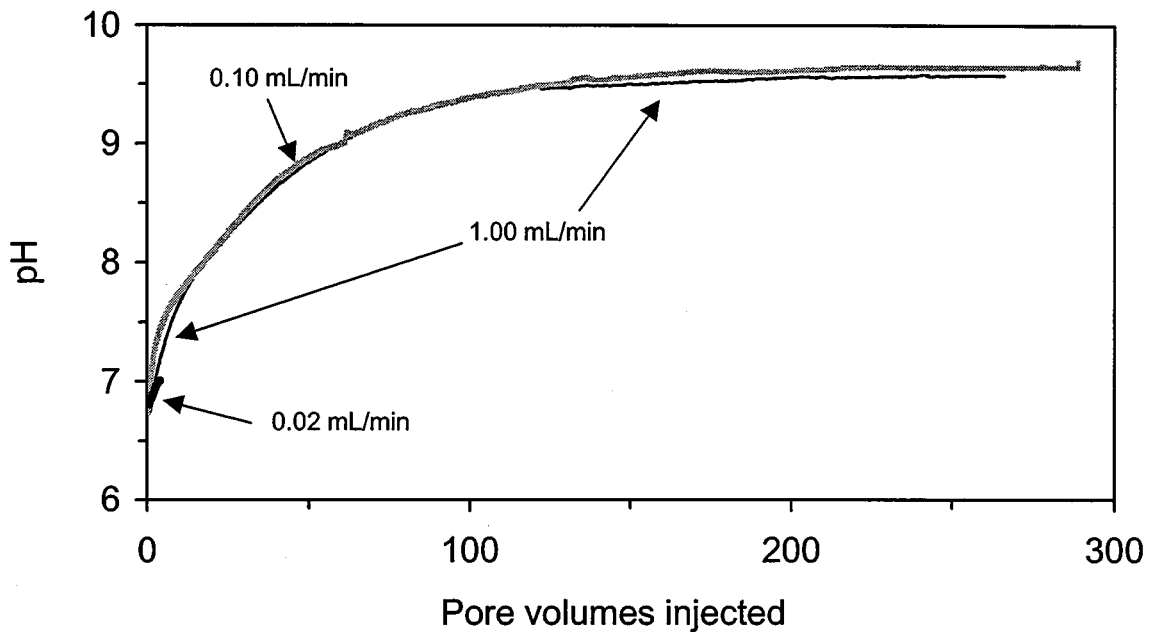


Figure 4.9 – Recovery of pH during injection of brine after contact with a chromium acetate solution.

the same pH as the chromium acetate solutions used in the flow experiments. The sodium acetate solution and KCl brine were alternately injected into the Bin#4 core for seven cycles. Each fluid was injected at a rate of 0.2 mL/min. for 120 minutes, which corresponded to 5.4 pore volumes injected per flow segment.

The pH of the effluent for each cycle is shown in Figure 4.10. The pH appeared to reach a steady state condition after seven cycles of injection. The pH ranged around the value of 9 during the injection of sodium acetate and brine solutions. These data were compared to the results in Figure 4.3 which was the same experiment but using chromium acetate instead of sodium acetate. This comparison showed that the buffering capacity of the acetate alone was not responsible for the pH level being around 7 that was observed during the injection of chromium acetate solutions in dolomite cores.

Summary

Chromium was retained during the propagation of chromium acetate solutions through dolomite rock. The amount of chromium retained increased with the residence time or shut-in time in the core. Retention was a function of time and not an equilibrium process. The mechanism causing retention did not limit the amount retained in the flow experiments.

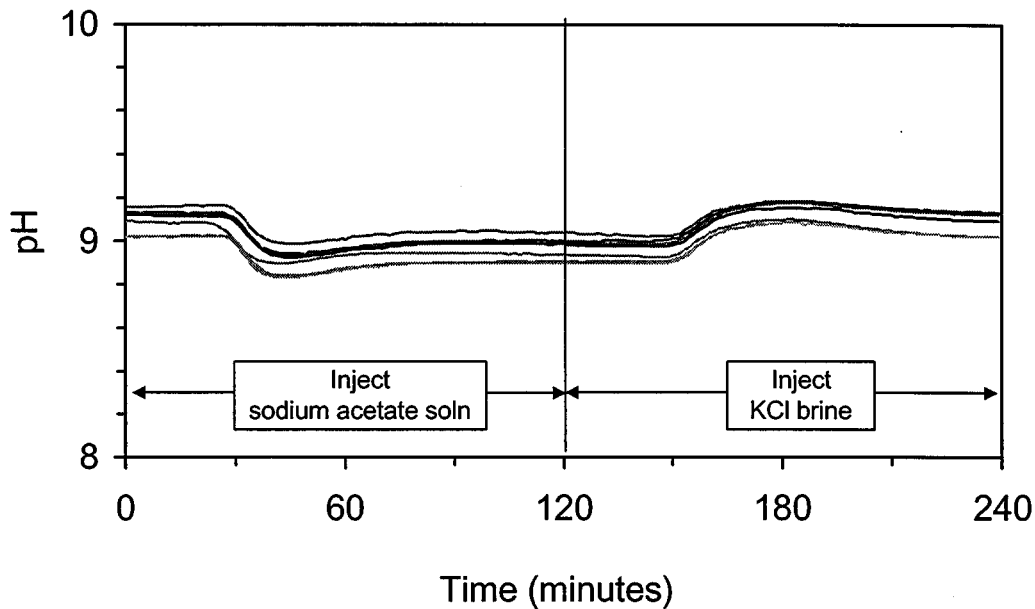


Figure 4.10 - Effluent pH during the injection of a sodium acetate solution; Core Bin #4.

The likely cause of chromium retention was precipitation at the elevated pH values the solution encountered in the core due to dolomite dissolution. Chromium acetate solutions reached a pH level of about 7 in the dolomite cores. This pH level was the result of dolomite dissolution and the interactions with the chromium acetate. The amount of chromium that can be retained by the precipitation mechanism for practical applications is almost limitless.

Chromium was retained faster in dolomite cores (presumably due to precipitation) than precipitation rates measured in bulk solutions [Zou et al.; 2000b]. The cause of the differences between the results of these types of experiments is not known.

The amount of KCl in the injected chromium acetate solution appeared to effect the rate chromium was retained in the dolomite cores. Experiments indicated that chromium retention was larger at higher KCl concentration.

References

1. McCool, C.S., Green, D.W., and Willhite, G.P., "Fluid/Rock Interaction Between Xanthan-Chromium(III) Gel Systems and Dolomite Core Material," *15, SPE Prod. & Facilities* (2000) 159.
2. Meister, J.J., "A Porous Permeable Carbonate for Use in Oil Recovery Experiments," *JPT* (November 1978) 1632.

3. Seight, R.S.: "Impact of Permeability and Lithology on Gel Performance," paper SPE/DOE 24190 presented at Eighth Symposium on Enhanced Oil Recovery, Tulsa, OK (22-24 April 1992).
4. Stavland, A., Ersdal, T., Kvanik, B., Lohne, A., Lund, T. and Vikane, O., "Evaluation of Xanthan-Cr Gels for Deep Emplacement: Retention of Cr (III) in North Sea Sandstone Reservoir," Seventh European Symposium on Improved Oil Recovery, Moscow, Russia (27-29 Oct. 1993).
5. Zou, B., McCool, C.S., Green, D.W., and Willhite, G.P., "A Study of the Chemical Interactions Between Brine Solutions and Dolomite," *SPE Reservoir Eval. & Eng.*, **3** (June 2000a) 209.
6. Zou, B., McCool, C.S., Green, D.W., and Willhite, G.P., "Precipitation of Chromium Acetate Solutions", *SPE Journal*, **5** (September 2000b) 324.
7. Welz, Bernhard, and Sperling, Michael: "Atomic Absorption Spectrometry", third completely revised edition, Wiley-Vch.

Chapter 5

Pressure Distribution and Fluid Displacement in Gels

Graduate Research Assistants: Xiaofang Suo and Joanne Sia Fen Fen

Introduction

Gelled polymer treatments are applied in oil reservoirs to improve fluid flow characteristics such that oil production is increased and/or water production is reduced. After placement, the gel is subjected to pressure gradients by flows of oil and water. Injected water imparts a pressure gradient on the gel after placement in the reservoir through an injection well. In applications adjacent to a production well, both oil and water flowing to the well subject the gel to a pressure gradient. Pressure gradients across the gel can result in the bulk displacement of the gel, rupture of the gel, or dehydration of the gel.

Al-Sharji et al. [1999] observed in micro-model experiments that water flowed through the polymer gel by diffusing into the gel structure, while oil flowed through gel in the form of immiscible drops or filaments which minimized the surface area of contact between the oil and the gel. Krishnan et al. [2000] demonstrated that chromium acetate-polyacrylamide gels dehydrated when subjected to pressure gradients by either oil or water. Water was squeezed out of the gel as the gel structure adjusted to the applied pressure gradient.

The objective of this work is to characterize the phenomena that occur when a confined length of gel is contacted by a pressurized fluid at one end. Experiments were conducted on a polyacrylamide-chromium(III) gel system in 8-foot and 5-foot long tubes (0.0625 inch ID). Brine and oil were used to exert pressure on the tubes. Fluid displacements and pressure distribution along the length of the gel were determined.

Experiment

Experiments were conducted on a gel system composed of polyacrylamide and chromium acetate. The gel system was prepared by mixing a stock polymer solution and a stock chromium solution in a 3:1 weight ratio. The polymer solution was prepared from Alcoflood 935 (Batch No. 7158V) at least 24 hours before gel mixing. The polymer stock solution contained 10,000 ppm polymer and 1.33% potassium chloride. The chromium solution was prepared from 50% chromium-acetate solution (Lot. No.40014806, McGean-Rohco. Inc. Date: 11/01/95) just prior to gel mixing. Concentration of chromium in the stock solution was 600ppm. The prepared gelant contained 7500 ppm polymer, 150 ppm chromium and 1% KCl. The pH of the freshly mixed gelant was about 4.8 and was adjusted to a pH of 5.0 using potassium hydroxide shortly after mixing. The gel time was approximately 15 hours at room temperature (about 24°C). The gel time was determined by measuring viscosity of a gelant sample as a function of time and was defined as the time at which the viscosity reached 200 cp.

After mixing and pH adjustment, the gelant was injected into tubes with an inside diameter of 0.0625 inches. The ends of the tubing and tee fittings were secured and the gelant solution was allowed to gel for 24 hours before application of pressure.

Two experiments were conducted: (1) oil and brine were used to exert pressure on an 8-foot long tube and (2) brine was used to exert pressure on a 5-foot long tube. The equipment setup for the experiments in an 8-foot long tube is shown in Figure 5.1a. A QUIZIX QL-700 Pump was used to apply brine or oil (viscosity of 38.8cP) at constant pressure to the gel tube system. The 8-foot long tube was divided into four 2-foot long sections that were separated by tee fittings. The gel tube outlet was closed, opened to the atmosphere or opened and placed in a 1% KCl solution. The pressure of the gel was measured at several positions along the tube using pressure transducers. The pressure lines between the transducers and gel tube system were filled with oil.

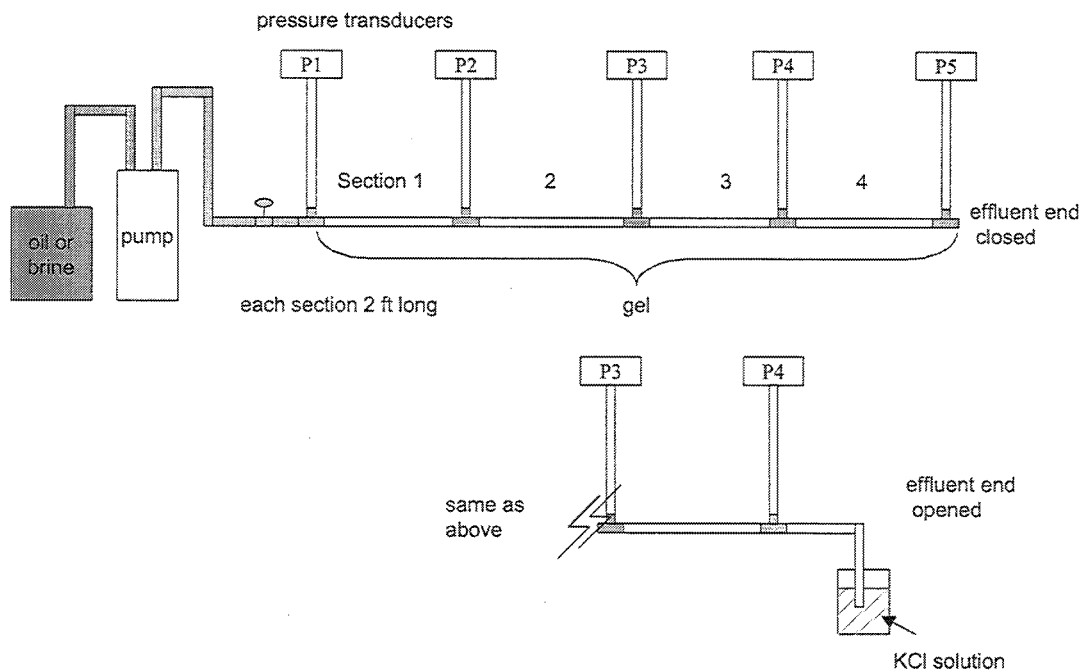
Several refinements were made in the procedures during the course of the experiment using oil to exert pressure. Evaporation of the gel at the effluent end of the gel tube occurred initially. One inch of the effluent end of the tube was cut and removed to eliminate the concentrated gel. The effluent end was then placed in water or 1% KCl solution to limit evaporation as shown in Figure 5.1a. Temperature control was improved during the experiment. The gel tube was placed in a constant-temperature water bath. Temperature control was further improved by enclosing the pump and pressure measuring equipment in a constant-temperature air bath.

The equipment setup for the experiment using brine to exert pressure on a gel in a 5-foot long tube is shown in Figure 5.1b. A transfer vessel containing brine was connected to the gel tube. The headspace of the transfer vessel was pressurized using nitrogen. Pressures along the gel were measured using transducers. The pressure lines were filled with oil.

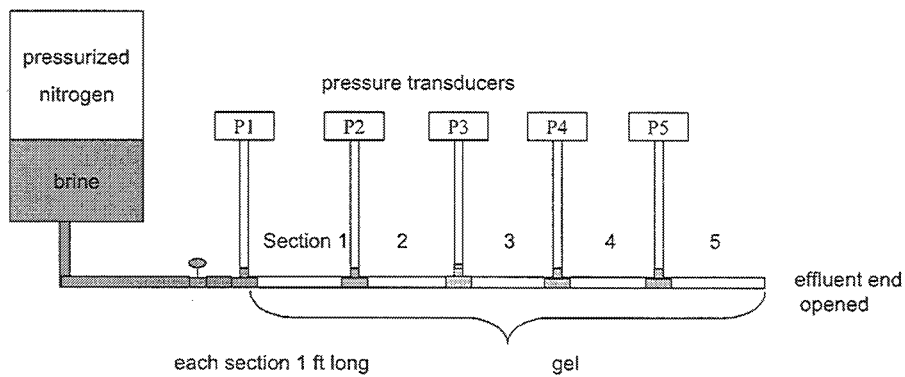
Results and Discussion

8-foot long gel tube. The objective of the first run in the 8-foot long tube was to determine the pressure distribution in the gel when pressure is applied at one end and the opposite end is closed to minimize fluid displacement in the tube. The gel tube was pressured using 1.0% KCl brine. Pressures measured along the gel tube are shown in Figure 5.2. Brine was applied at a 46 psi pressure then increased to 65 and 88 psi and then back to 68 psi in steps over about a 20 hour time period as shown by pressure P1. The final 68 psi pressure was applied for about an hour followed by the closure of a valve between the pump and the gel tube at 20 hours. The valve was closed to test the system for leaks. The pressure decreased slowly over a 28-hour period to 28 psi indicating a small leak. The inlet valve was opened to the atmosphere and the pressure at the inlet (P1) decreased to 0 psi at the 48-hour mark.

Pressure P2, that was measured two feet from the inlet, showed a small response to the applied pressures during the first 48 hours. Pressure P2 decreased slowly after the inlet pressure was reduced to zero at 48 hours. No significant pressure response was observed at transducers P3, P4 and P5. Daily changes in the room temperature affected the pressures measured at all of the positions along the tube. A small hump between 20 and 24 hours was observed for all the pressures as shown in Figure 5.2. This hump was repeated every 24 hours indicating that the cause was daily temperature fluctuations in the laboratory.



(a) Experiments in 8-foot long tube.



(b) Experiment in 5-foot long tube.

Figure 5.1 – Schematic of equipment used for subjecting gels to a pressure gradient.

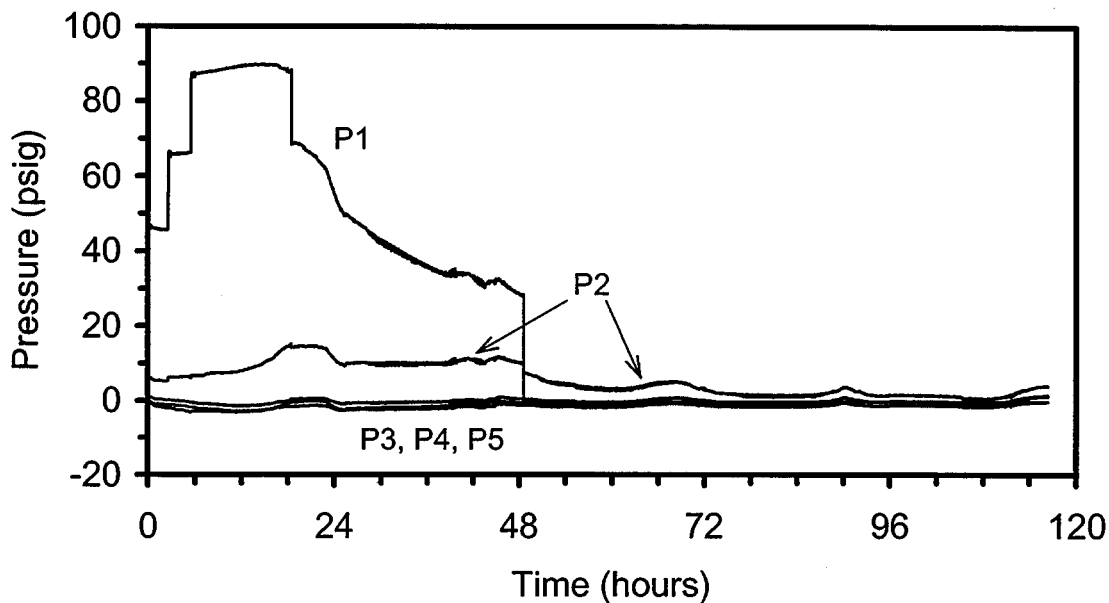


Figure 5.2 – Pressures measured along the length of the gel-filled tube when pressure is applied to one end with brine and the opposite end of the tube is closed.

The results of this run clearly show that the gel in the tube did not fully transmit pressure along its length during the 48-hour period when the outlet of the tube was closed. A moderate increase in pressure was observed two feet down the tube while no pressure transmission was observed at four feet or greater distances down the tube.

The objective of the second run in the 8-foot long tube was to observe fluid displacement and pressure response when the inlet of the tube was subjected to pressure and the outlet of the tube was open. Oil was used to apply pressure in this run. The oil was dyed red in order to observe fluid displacements.

Oil was applied to the inlet of the gel tube at a pressure of about 80 psig. The pressure applied at the inlet, P1, and the pressures measured along the length of the gel tube are shown in Figure 5.3. Fluctuations in the pressures were the result of daily variations in room temperature. Placement of the gel tube in a constant-temperature water bath at about 350 hours did not suppress the pressure fluctuations. However, construction of a constant-temperature air bath to enclose the pump and pressure measuring system

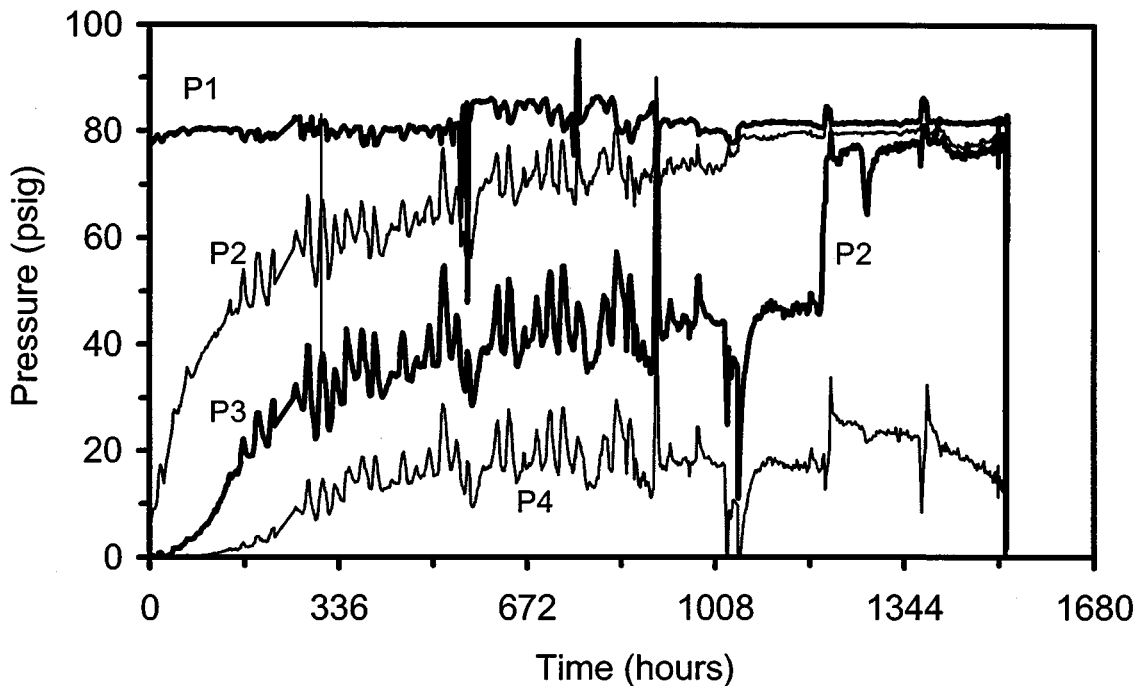


Figure 5.3 – Pressures measured along the length of the gel-filled tube when pressure is applied to one end with oil and the opposite end of the tube is open.

beginning at about 1050 hours provided better control of temperature-induced effects. Thereafter, only two temperature excursions occurred, at 1200 and 1380 hours, due to room temperatures exceeding 30°C.

Neglecting the temperature-induced pressure fluctuations, pressures at P2, P3 and P4 increased gradually during the first 500 hours resulting in a nearly linear pressure gradient along the tube. During this time and up to about 1050 hours, oil gradually penetrated through Section 1. A schematic of the oil distribution in Section 1 at this time is shown in Figure 5.4. Oil had displaced some of the gel at the entrance. A series of oil drops were distributed in the gel along the center of the tube. The drops were smaller in size towards the entrance. A large drop was observed at the furthest distance that oil had penetrated downstream. The volume of the large drop increased in volume as it progressed through the section. The oil drops were always static when observed. The actual movement of the drops was not observed, only inferred by their progressive positions at discrete times. It was suspected that a narrow channel in the center of the gel connected the drops and that oil flowed through this channel when movement occurred. (This channel was observed at the end of the experiment after oil broke through to the end of the tube and oil continuously flowed through the system.) During the static periods, it is suspected that segments of the channel collapse between the oil drops that form due to the elasticity of the gel and the interfacial tension between the oil and the gel. It was also suspected that the gel

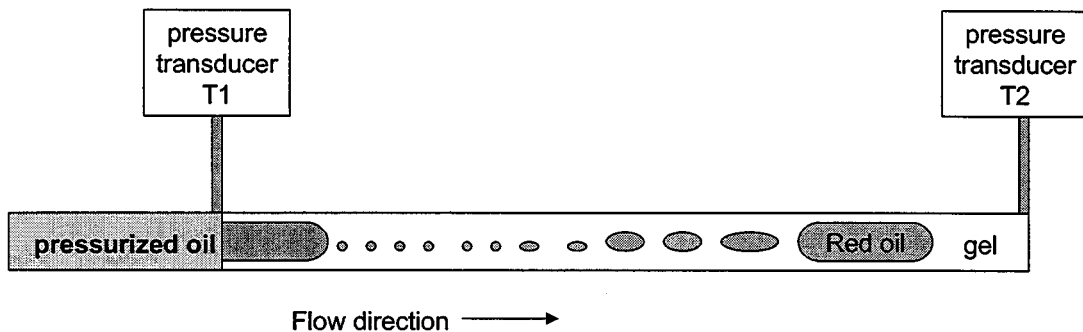


Figure 5.4 – Schematic of the oil distribution in the gel in Section 1 of the tube.

dehydrated, or expelled solvent, during the displacement of oil through the tube. However, the presence of expelled solvent was not observed, probably due to the small volume that was expected to be expelled and/or the difficulty of differentiating between gel and solvent in the small tube.

Oil distributions observed later in other sections were similar to those observed in Section 1, except the drops were not as uniform or as ordered. An exception occurred in Section 2 after the oil front penetrated a portion of Section 3. No oil drops were observed in Section 2. Oil displacement through Section 2 was assumed to occur through a small oil channel in the center of the gel. In general, oil displacement through the gel tube did not show uniform behavior through the length of the tube. Displacement was complex and probably was affected by minor inhomogeneities in the gel structure.

The pressure at P2 approached the value of P1, the applied pressure, as oil moved into Section 2 at 1050 hours (Figure 5.3). Oil progressed through Section 2 and moved into Section 3 at 1200 hours when the pressure at P3 jumped from 46 to 75 psi. This oil movement and pressure response occurred at the same time as a temperature excursion occurred in the laboratory. It is unknown if they are related.

Oil penetrated only about half way through Section 3 during the period between 1200 and 1510 hours. The pressure drop across Section 3 (the difference between P4 and P3) during this time was about 60 psi (Figure 5.3). Between 1510 and 1537 hours, oil progressed through the second half of Section 3, through Section 4 and out the end of the tube. Oil penetrated the gel at a much faster rate at the end of the tube. The rate oil was injected into the tube was recorded by the pump software and is presented in Figure 5.5 for the time period between 1520 and 1537 hours. Oil broke through to the end of the gel during the night and the exact time was not observed. Several spikes in the flow rate between 1526 and 1528 hours indicated the oil surged before a steady stream was developed through the gel at 1528.4 hours. During the oil surges, a major portion of the total pressure drop (~70psi) moved erratically between Sections 2, 3 and 4. After the steady stream of oil developed at 1528.4 hours, small pressure drops were observed in Sections 2 and 4 and steady pressure drops of 20 and 60 psi were observed in Sections 1 and 3, respectively. The oil reservoir for the pump was depleted at 1537 hours and the pump shut down.

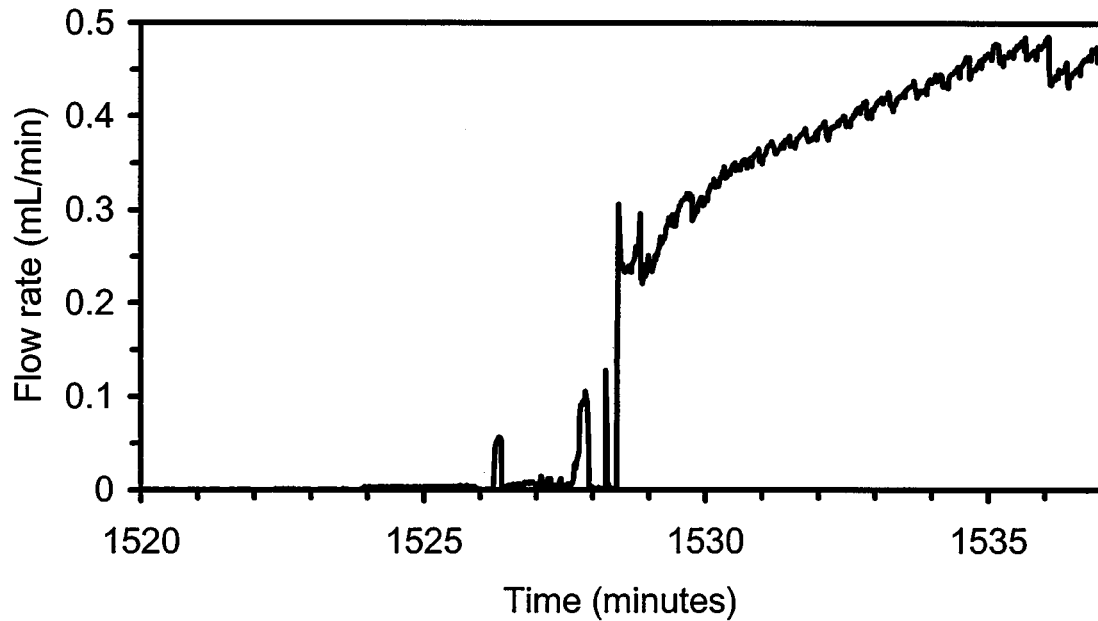


Figure 5.5 – Flow rate of oil during the period of time when oil penetrated the entire length of the gel.

The second run in the 8-foot long tube demonstrates that oil can penetrate and develop channels through a gel. Oil displacement through the gel occurs intermittently. During static periods, the oil forms a series of drops in the gel along the center of the tube. For the conditions used in this run, it took over two months for the oil to penetrate the entire length of the gel in an 8-foot long tube.

5-foot long gel tube The objective of the run in the 5-foot long tube was to determine the pressure distribution in the gel when pressure is applied at one end of the tube using brine and the opposite end of the tube is open. Pressures measured along the gel during the experiment are shown in Figure 5.6. A pressure of 90 psig was applied for about 20 hours and then increased to 170 psig for about 40 minutes as shown by pressure P1 in the figure. The applied pressure was not transmitted along the gel during the application of these pressures as indicated by the near zero values of P2, P3, P4 and P5. P2 was measured one foot downstream of the tube inlet. Brine penetrated about six inches into the gel during this time period. The brine formed a couple of "drops" in the center of the tube, enclosed by gel. The brine was dyed red in order to differentiate between brine and gel.

The pressure on the brine transfer cylinder was released for about five minutes (0 psig). This was followed by the pressurization of the cylinder to 240 psig with nitrogen. Brine penetrated the gel at this pressure and developed a channel through the entire length over the next 75 minutes. Pressures measured along the gel changed abruptly during channel development. After the

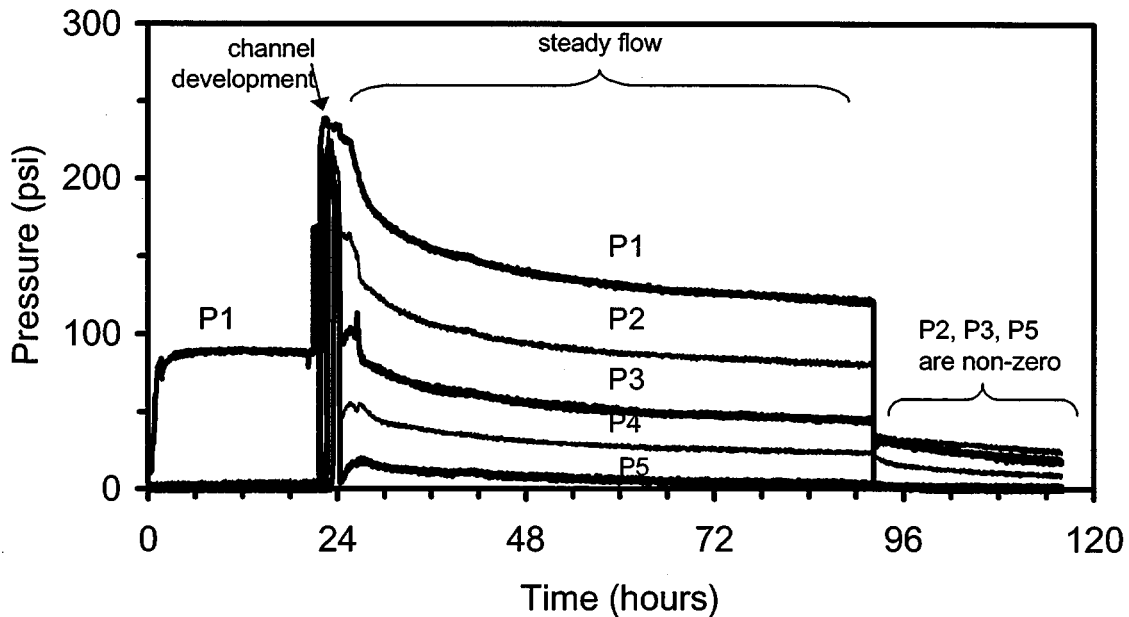


Figure 5.6 – Pressures measured along the length of the gel-filled tube when pressure is applied to one end with brine and the opposite end of the tube is open.

channel was formed, brine steadily flowed through the tube at an average flow rate of about 0.7 mL/hr during the time period between 25 and 92 hours (Figure 5.6). An approximately linear pressure gradient along the tube was observed during the steady flow of brine. The applied pressure decreased during this period as the nitrogen in the transfer vessel expanded to displace the brine.

The pressure data during the time period when the brine penetrated the gel and developed channels are shown in Figure 5.7. When the pressure on the brine was increased to 240 psig at 21.8 hours, a brine "drop" that was in Section 1 quickly penetrated and stopped in Section 2. This movement corresponded to the abrupt increase of pressure P2. Pressure P2 decreased (cause unknown) and then increased with pressure P3 at 22.7 hours. Movement of brine drops through the remaining length of the tube correlated with the abrupt increases observed in pressures P3, P4 and P5 (Figure 5.7). The furthest penetrating brine drop was about 3 to 5 inches from the each pressure port when the abrupt pressure increase occurred. That is, a significant portion of the pressure drop applied to the tube is localized at a point just ahead of the furthest position that the pressurizing fluid had advanced. The localized pressure gradient in some manner alters the gel structure, which then allows the pressurizing fluid to advance. This observation may indicate that the length of the gel downstream of this zone may not have a significant influence on the process. Further investigation is required to determine the mechanisms responsible for fluid movements through gels.

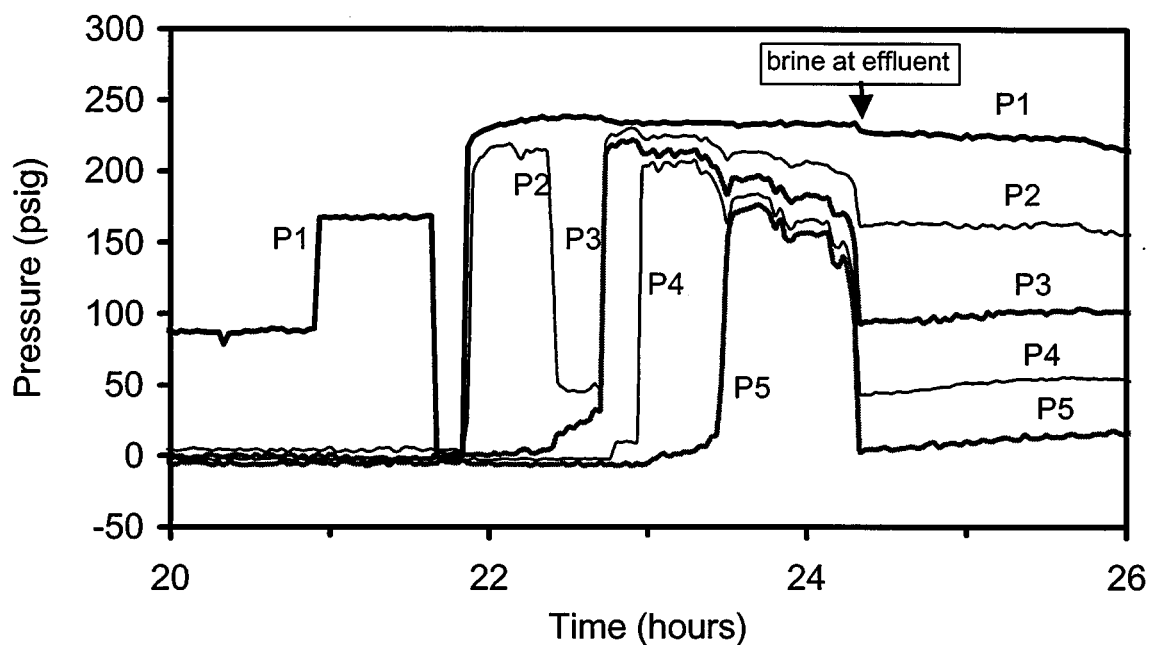


Figure 5.7 – Pressures measured along the length of the gel-filled tube during the time period when brine developed channels through the gel.

Summary

These initial experiments have demonstrated that both oil and brine develop channels and flow through gels. The movement of oil and brine through the gel occurs intermittently. Small pressure gradients were observed along the gel where the brine or oil had penetrated. Most of the applied pressure gradient was in the gel downstream of the position where the oil or brine had penetrated. Data indicated a sharp pressure gradient over a small segment in the downstream gel. The process is complex and mechanisms are not apparent.

Channel development through gels has implications on the performance of gelled polymer treatments. In production wells, injected brine can develop channels through the placed gel, possibly reducing the effectiveness of the treatment. In production wells, the relative development of channels by oil and water could affect the treatment's ability to reduce water production while sustaining oil production.

Future Work

Experimental procedures are being developed to characterize the phenomena that occur when a confined length of gel is subjected to a pressurized fluid. Further refinements in the procedures will be developed particularly methods to determine fluids and flow rates at the effluent end. The effect of tubing diameter, tubing length, injection pressure and injection liquid (brine or oil) on the progression of pressurized fluids through gels will be investigated. The objective of these experiments is to determine generalized mechanisms that are responsible for channel development.

References

1. Al-Sharji, H. H., Grattoni, C. A. Dawe, R.A. and Zimmerman, R.W.: "Pore-Scale Study of the Flow of oil and Water through Polymer Gels", paper SPE 56738 presented at the 1999 SPE Annual Technical conference and Exhibition held in Houston, TX (3-6 October 1999).
2. Krishnan,P., Asghari, K., Willhite, G.P., McCool, C.S., Green, D.W. and Vossoughi, S.: "Dehydration and Permeability of Gels Used in In-situ Permeability Modification", paper SPE 59347, presented at the 2000 SPE/DOE Improved Oil Recovery Symposium held in Tulsa, OK (3-5 April 2000).

Chapter 6

Technology Transfer

Presentations

“Dehydration and Permeability of Gels Used in In-situ Permeability Modification”, C.S. McCool, paper SPE 59347, presented at the 2000 SPE/DOE Improved Oil Recovery Symposium held in Tulsa, OK, 3-5 April 2000.

“Mechanisms Causing Disproportionate permeability in Porous Media Treated with Chromium Acetate/HPAAM Gels,” G.P. Willhite, paper SPE 59345, presented at the 2000 SPE/DOE Improved Oil Recovery Symposium held in Tulsa, OK, 3-5 April 2000.

Papers and Publications

Zou, B., McCool, C.S., Green, D.W., and Willhite, G.P., “A Study of the Chemical Interactions Between Brine Solutions and Dolomite,” *SPE Reservoir Eval. & Eng.*, 3 (June 2000) 209.

Krishnan, P., Asghari, K., Willhite, G.P., McCool, C.S., Green, D.W. and Vossoughi, S.: “Dehydration and Permeability of Gels Used in In-situ Permeability Modification”, paper SPE 59347, presented at the 2000 SPE/DOE Improved Oil Recovery Symposium held in Tulsa, OK (3-5 April 2000).

Willhite, G.P., Zhu, H., Natarajan, D., McCool, C.S. and Green, D.W., “Mechanisms Causing Disproportionate permeability in Porous Media Treated with Chromium Acetate/HPAAM Gels,” paper SPE 59345, presented at the 2000 SPE/DOE Improved Oil Recovery Symposium held in Tulsa, OK (3-5 April 2000).

